UPTEC W06 014
Examensarbete 20 p
Maj 2006

Snow Interception Measurements using Impulse Radar

Snöinterceptionsmätningar med impulsradar

Jan Magnusson

Abstract

Snow Interception Measurements using Impulse Radar

Jan Magnusson

Interception of rain or snow in forest canopies is an important component of the hydrological cycle. Up to one third of the total winter precipitation never reaches the ground in forest areas due to evaporation losses of intercepted snow, which reduces spring-time water flow in rivers. Accurate spring flow predictions are important for the hydro-power industry. Appropriate measurement methods of intercepted snow are needed in order to improve models involving the interception evaporation process. The aim of this study was to explore the possibilities of an impulse radar system to measure the snow interception storage on coniferous trees. The method is based on measurements of the velocity and attenuation of an electromagnetic impulse wave, generated in a transmitting antenna and sent through a forest section and detected by a receiving antenna. The attenuation and velocity is affected by ice and water in the canopy air space, and can be related to amounts of water using so-called mixing formulas that describe the average electromagnetic properties of heterogeneous materials. Controlled laboratory measurements on small canopies showed that interception of liquid water was well above the detectable limits of the radar system, with respect to both attenuation and velocity changes. Estimations of the mass of intercepted water based on velocity changes overestimated the reference measurements, but relative variations were well captured. No clear relation could be found between amount of water on canopies and impulse wave attenuation from the experiments. The attenuation results were difficult to interpret, and appropriate mixing formulas were not found in the literature. The method was further tested for one week under field conditions in northern Sweden. In spite of a non-optimal equipment installation results of estimated changes of the interception storage showed a good agreement with observed weather variations and reference measurements using a tree weighing device. The method can have good conditions to give correct estimations of the snow interception storage, using appropriate installation and further calibration measurements.

Keywords: Interception, snow, ground penetrating radar, mixing formulas.

Referat

Snöinterceptionsmätningar med impulsradar

Jan Magnusson

Interception av snö eller regn på trädkronor är en viktig del av det hydrologiska kretsloppet. Upp till en tredjedel av all snö som faller över skogsområden når aldrig marken på grund av stora avdunstningsförluster av interceptionsförrådet, vilket minskar vårflöden i älvar. Goda prognoser av dessa flöden är viktiga för vattenkraftsindustrin. För att kunna förbättra modeller, i vilka interceptions-avdunstningsprocessen ingår, krävs lämpliga mätmetoder för interceptionförrådet av snö. Syftet med detta arbete var att undersöka om impulsradarutrustning kan användas för att mäta interceptionsförrådet av snö på barrträd. Metoden bygger på att mäta hastigheten och utsläckningen hos en elektromagnetisk impulsvåg, vilken skickas från en sändarantenn genom ett avsnitt skog till en mottagarantenn. Både utsläckningen och hastigheten påverkas av snö och vatten på trädens kronor, och kan med så kallade blandningsformler relateras till mängd vatten. Blandningsformler beskriver de elektromagnetiska egenskaperna hos heterogena material. Laboratorietester visade att interception av flytande vatten på små trädkronor gav upphov till förändringar av impulsvågens hastighet och utsläckning mätbara med radarutrustningen. Uppskattningar av mängden intercepterat vatten från radarmätningarna gav en överskattning jämfört med oberoende referensmätningar, däremot stämde relativa variationer väl överens mellan mätningarna. Tydliga samband mellan impulsvågens utsläckning och mängden intercepterat vatten kunde inte bestämmas från experimenten. Utsläckningsresultaten var svårtolkade och lämpliga blandningsformler hittades inte i litteraturen. Metoden testades även en vecka i fält i norra Sverige. Trots att installationen inte var den bästa visade resultaten ändå god överensstämmelse mellan uppskattade förändringar av interceptionsförrådet från radarmätningarna, och observerade väderförändringar samt oberoende referensmätningar med en trädvågsanordning. Resultaten tyder på att metoden kan ge goda uppskattningar av interceptionsförrådet, då en väl fungerande installation av utrustningen används och efter att vidare kalibreringsförsök genomförts.

Nyckelord: Interception, snö, ground penetrating radar, blandningsformler.

Department of Earth Sciences, Uppsala University
Villavägen 16
752 36 Uppsala, Sweden

ISSN 1401-5765

Preface

This thesis work was done for the Department of Land and Water Resources Engineering (Royal Institute of Technology, KTH) and is a part of a M.Sc. Education in Aquatic and Environmental Engineering at Uppsala University.

Supervisor:	David Gustafsson Land and Water Resources Engineering Royal Institute of Technology, KTH
Subject reviewer:	Sven Halldin Institute of Earth Sciences Uppsala University

I want to give a special thanks to Ola Wessely for bringing light to the often confusing subject of electromagnetic field theory. Christer Gustafsson at Raycon (Malå, Sweden) deserves gratitude for providing facilities and material for the experiments in Malå. Thanks to Angela Lundberg for lending the tree weighing device for intercepted snow during the field test. Foremost, none of this would have been possible without the dedication to snow from David Gustafsson, thanks for all commitment and supervision. It was a very nice last half year at school.

UPTEC W06 014, ISSN 1401-5765
Printed at the Department of Earth Sciences, Geotryckeriet, Uppsala University, Uppsala, 2006.

Table of Contents

1. Introduction

Interception is the part of rain or snow falling on and caught by vegetation canopies, and is an important component of the hydrological cycle. Snow on trees is more exposed to radiation and wind compared to snow on the ground, giving high evaporation losses. In spite of low temperatures, up to one third of the total winter season precipitation never reaches the ground in forest areas due to evaporation of intercepted snow (Hedstrom & Pomeroy, 1998). This has a major impact on the snowpack development, and the maximum snow water equivalent on the ground. Throughfall, in other words the snow and water reaching the ground, can eventually contribute to the ground water and streams. In large boreal forest areas the spring flow size is reduced compared to unforested areas due to evaporation of the snow on trees. It has been shown that clear-cutting forest increases the water yield (Bosch & Hewlett, 1982; Sahin & Hall, 1996). Correct spring flow predictions is of importance to the hydro-power industry among others. Also the structure of the snowpack is changed under trees and is crucial for avalanche formation and protection in sub-alpine forest regions (Pfister & Schneebeli, 1999). Recently, the interception process has become of interest also for meteorological research due to its influence on the atmosphere-land surface heat exchange (Essery *et al*., 2003). Furthermore, global warming could disrupt today balance leading to a water budget change in cold regions, and the relative impact of snow interception compared to other water budget components may change. Modeling and understanding of interception processes are important and of interest for all these reasons and aspects.

Lundberg (1993) states some criteria on an ideal measurement method for snow interception, necessary in oder to model fluxes and processes governed or influenced by intercepted snow:

- Negligible disturbances from the measurement equipment.
- Applicable during all weather conditions and environments.
- High time resolution, at least measurements once every hour.
- Determining the interception storage with an accuracy of at least 0.01 mm water equivalent per square meter, and giving representative estimations over a forest stand.

There are several methods to estimate or measure the amount of snow on forest canopies. Many of those methods rely on other measured values than the actual snow interception storage. For example, the total interception storage over a season can be estimated from the difference between the snow accumulation on the ground and evaporation in a forest, and on a open field (Lundberg & Halldin, 2001). The amount of new-fallen snow under canopies in a forest and on a clearing in the vicinity gives an estimate of the instant interception storage (Hedstrom & Pomeroy, 1998; McNay *et al*., 1988). All these methods are mass-balance determinations, which have a number of drawbacks such as relative low accuracy and poor time resolution. Numerical interception models are often used in combination with mass-balance estimates to increase the accuracy and time resolution. In these models other measurements are used as complements, such as the radiation, temperature or snow density (Lundberg & Halldin, 2001).

Lundberg (1998) presents two approaches for direct determination of the snow amount on canopies, without using other measured values. Weighing a single full-size tree is one way giving continuous measurements of the intercepted snow. The method can not be used in a dense forest due to branches from other trees disturbing the measurement. Translating the weighted amount of snow on a single tree to an interception storage of a forest stand is difficult and gives uncertain results. A second method for direct determination of the amount of snow on canopies is to measure gamma-ray attenuation through a forest section. The gamma rays are attenuated in relation to the amount of snow or ice on the trees. By raising and lowering the source and detector, both always on

the same elevation, a vertical profile of the intercepted snow mass can be determined. Integration of the values over the profile gives the interception storage with an accuracy as high as approximately 0.1 mm water equivalent per square meter. The use of a radioactive source and the high maintenance efforts makes the method unsuited for a standard field scale measurement procedure.

Bouten (1991) measured the extinction of continuous microwaves to quantify rain interception. A transmission measurement (Figure 1) was used similar to the gamma-ray attenuation method. In a transmitter antenna a continuous electromagnetic wave was generated and sent through a forest section and detected by a receiving antenna. The wave energy attenuation increases when water is present since electromagnetic waves induces currents in conducting media, and thereby creates heat,. The microwave attenuation was related to an amount of water on the canopies using calibration measurements. According to Bouten this method can only be used to measure interception of liquid water (Lundberg, 1993).

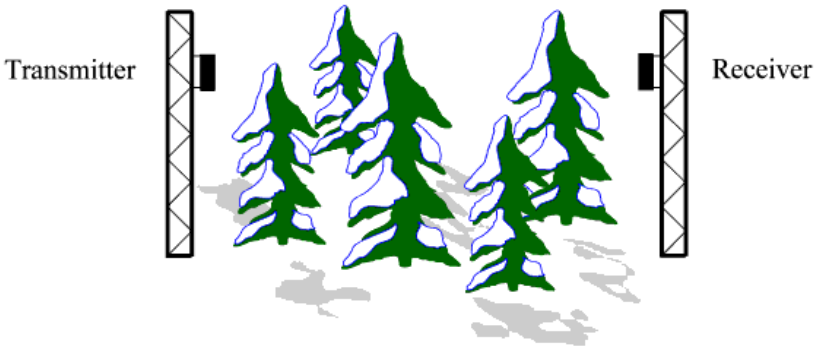

Figure 1. *Schematic illustration of a transmission measurement through a forest section.*

All existing methods for snow interception measurements have certain drawbacks, as for example low accuracy or poor time resolution. New approaches are thus needed in order to improve models involving the interception evaporation process further.

Impulse radar is a geophysical method which has been used in several applications to map different snow and ice conditions on or below the ground surface, for example determining the thickness of a snowpack (Albert *et al*., 1999; Bruland, 2002). Typically, so-called ground penetrating radar (GPR) systems are used for these surveys. The principle is simple; travel time and amplitude change of a short electromagnetic impulse wave is measured between a transmitter and a receiver antenna. The most common application of this technique is to have both antennas positioned at the ground surface facing downwards, measuring reflections of the radar wave from objects below. In this case, the travel time of radar impulse wave can be used to determine the depth to the reflecting object as long as the propagation velocity is known. Impulse radar is also used in transmission constellation, particularly in borehole investigations of bedrock properties. In this configuration with a known distance between the antennas, it is rather straight forward to estimate velocity and attenuation of the radar wave from the travel time and amplitude change. The velocity and attenuation of the radar wave gives useful information about the medium between the antennas. Principally, there are no limitations of using a GPR system in transmission mode above ground for snow interception measurements, an application so far unexamined. Compared to the microwave method presented above this technique gives one additional measurement parameter, the impulse wave velocity, which similar to the attenuation can be related to the amount of snow or water on the canopies.

The overall aim of this study was to investigate the possibilities to use GPR system to measure snow interception on coniferous forest stands (Figure 1). Three specific objectives were formulated:

- To compile theoretical and empirical knowledge on the propagation of electromagnetic

waves, and electromagnetic material properties, which can be used to quantify interception of snow or rain on tree canopies from radar measurements.

- To test the GPR system and the theoretical model under controlled laboratory conditions.
- To briefly test the equipment in field for a forest stand interception measurement and compare the results against an independent estimation of the interception storage.

2. Materials and methods

2.1. Electromagnetic field theory applied for impulse radar measurements

The GPR equipment generates electromagnetic impulse waves. A theoretic approach to analyze the propagation of an impulse wave, the velocity and attenuation, can be derived using Maxwell's equations.

2.1.1. Maxwell's equations and constitutive relations

Electromagnetic field quantities can be described by Maxwell's equations. These equations state the interaction between the electric and magnetic fields. Eq. (1) shows that a time varying magnetic flux $\boldsymbol{B}$ generates an electric field $\boldsymbol{E}$. In the other direction, eq. (3) states that a time varying electric flux $\boldsymbol{D}$ or a static current $\boldsymbol{J}$ gives rise to a magnetic field $\boldsymbol{H}$. The relations (2) and (4) express the physical principles of the existence of free electric charges ρ_f working as sources for electric fluxes, and the opposite, the non-existence of magnetic point charges.

$$\nabla \times \boldsymbol{E} = -\frac{\partial \boldsymbol{B}}{\partial t} \tag{1}$$

$$\nabla \cdot \boldsymbol{D} = \rho_f \tag{2}$$

$$\nabla \times \boldsymbol{H} = \boldsymbol{J} + \frac{\partial \boldsymbol{D}}{\partial t} \tag{3}$$

$$\nabla \cdot \boldsymbol{B} = 0 \tag{4}$$

A set of constitutive equations for the traveling medium response to the electromagnetic fields can be stated if the traveling medium is assumed to be isotropic and homogeneous, in other words a medium with the same properties everywhere independent of the traveling direction. These equations relate the different field quantities to one another by the following material constants: the dielectric permittivity ε, magnetic susceptibility μ and conductivity σ (Annan, 2003).

$$\boldsymbol{D} = \varepsilon \boldsymbol{E} \tag{5}$$

$$\boldsymbol{B} = \mu \boldsymbol{H} \tag{6}$$

$$\boldsymbol{J} = \sigma \boldsymbol{E} \tag{7}$$

The assumption of a homogeneous isotropic medium is especially useful if formulas are available to describe the electromagnetic material properties in terms of physical characteristics such as water content.

2.1.2. Velocity and attenuation of impulse waves

Every medium has certain electromagnetic properties, determining the velocity and attenuation of an electromagnetic wave traveling through it. These characteristics can be estimated if the speed and attenuation of the electromagnetic wave is known. In order do this in a practical useful way some assumptions, both on the impulse wave and on the traveling medium, must be used. The approach presented in this section can be found in every textbook concerning basic electromagnetic field theory, for example Wangsness (1986), and is often used for evaluating GPR surveys.

By combining the constitutive relations and Maxwell's equations one can see that oscillating electric charges, as in a radar antenna for example, generates a time varying magnetic field, which induces an electric field. A sinusoidal electromagnetic wave propagating through space is thereby created (Young & Freedman, 2000). In this following section the spreading of such a wave in a homogeneous isotropic medium is considered.

If only very small amounts of free charges ρ_f exist they can be neglected. The magnetic field and the electric current can then be eliminated from eq. (3) using eqs. (5) and (7). Multiplying the result with eq. (6) gives an equation describing the behavior of the electric field in relation to the magnetic flux for the electromagnetic wave.

$$\nabla \times \boldsymbol{B} = \mu \sigma \boldsymbol{E} + \mu \varepsilon \frac{\partial \boldsymbol{E}}{\partial t} \tag{8}$$

To simplify the above expression to a function that only depends on the material constants and the electric field Wangsness (1986) uses the following derivation step; the curl[1] of eq. (1) and the rotation of the magnetic flux is substituted with eq. (8). This result is again simplified by neglecting the free charges ρ_f, which implies that the dot product[2] of the gradient and the electric field is zero. The propagation of the electric field component of the electromagnetic wave is then described by the following vector valued partial differential equation.

$$\nabla \times (\nabla \times \boldsymbol{E}) = \nabla (\nabla \cdot \boldsymbol{E}) - \nabla^2 \boldsymbol{E} = -\nabla^2 \boldsymbol{E} = -\mu \sigma \frac{\partial \boldsymbol{E}}{\partial t} - \mu \varepsilon \frac{\partial^2 \boldsymbol{E}}{\partial t^2} \tag{9}$$

Now, considering eq. (9) and taking $\boldsymbol{E}$ in just one of its rectangular components it turns into a scalar function $\Psi(z,t)$**,** where z is the position and t is time, used in the following expression:

$$\frac{\partial^2 \Psi(z,t)}{\partial z^2} - \mu \sigma \frac{\partial \Psi(z,t)}{\partial t} - \mu \varepsilon \frac{\partial^2 \Psi(z,t)}{\partial t^2} = 0 \tag{10}$$

A solution, eq. (11), can be stated to the expression above if the wave is treated as constant on any plane perpendicular to the traveling direction, called a plane wave, and only sinusoidal, harmonically varying with time. The angular frequency ω is restricted to be real and positive and k is called the dispersion constant.

$$\Psi(z,t) = \Psi_0 \, e^{i(kz - \omega t)} \tag{11}$$

---

1 $\boldsymbol{A} \times \boldsymbol{B} = (A_y B_z - A_z B_y)\hat{\boldsymbol{x}} + (A_z B_x - A_x B_z)\hat{\boldsymbol{y}} + (A_x B_y - A_y B_x)\hat{\boldsymbol{z}}$ (Curl or rotation)

2 $\boldsymbol{A} \cdot \boldsymbol{B} = A_x B_x + A_y B_y + A_z B_z$ (Scalar, dot product)

$$k^2 = \omega^2 \mu \varepsilon + i \omega \mu \sigma \tag{12}$$

Strictly, this solution and the steps leading to it, as presented by Wangsness (1986), is only valid for one specific wave frequency if material constants are frequency dependent. However, in the frequency range that most GPR systems operate (~10MHz-1GHz) this solution can be assumed to be valid due to the small constant changes within it (Annan, 2003). This frequency range is known as the GPR plateau (Annan, 2003). By the assumptions made for the solution of eq. (10), the dispersion constant k can be written as a function of the two variables α and β:

$$k = \pm(\alpha + i\beta) \tag{13}$$

Wangsness (1986) substituted eq. (13) in eq. (12), and separated the real and imaginary part, and solved the resulting equation system giving two expression for α and β, eqs. (14) and (15), respectively. The low loss criteria, implying $\sigma \ll \varepsilon\omega$, is commonly used in GPR contexts (Annan, 2003). Both the expression for α and β can then be simplified. For α the second degree division in eq. (14) can be omitted. In the eq. (15) for β the square root containing the second degree division is approximated with a Taylor expansion and all higher degree terms are neglected.

$$\alpha = \omega \sqrt{\frac{\mu \varepsilon}{2}} \left(\sqrt{1 + \left(\frac{\sigma}{\omega \varepsilon} \right)^2} + 1 \right)^{1/2} \simeq \omega \sqrt{\mu \varepsilon} \tag{14}$$

$$\beta = \omega \sqrt{\frac{\mu \varepsilon}{2}} \left(\sqrt{1 + \left(\frac{\sigma}{\omega \varepsilon} \right)^2} - 1 \right)^{1/2} \simeq \frac{\sigma}{2} \sqrt{\left(\frac{\mu}{\varepsilon} \right)} \tag{15}$$

Replacing the dispersion constant in eq. (11) with eq. (13) and separating α and β in the exponential gives a first term describing the wave speed and a second term describing the wave attenuation.

$$\Psi(z,t) = \Psi_0 \, e^{i(\alpha z - \omega t)} \, e^{-\beta z} \tag{16}$$

For $\Psi(z,t)$ to be a real valued function, the first exponential term must equal unity implying that $\alpha z - \omega t = 0$. Thus, an equation of the impulse wave speed can be derived:

$$v = \frac{z}{t} = \frac{\omega}{\alpha} = \frac{1}{\sqrt{\mu \varepsilon}} \tag{17}$$

If no ferromagnetic materials are present the magnetic susceptibility is unity and the equation for the electromagnetic wave velocity becomes:

$$v = \frac{1}{\sqrt{\mu \varepsilon}} = \frac{1}{\sqrt{\varepsilon_0 \varepsilon_r}} = \frac{c}{\sqrt{\varepsilon_r}} \tag{18}$$

where the dielectric permittivity is rewritten as the dielectric permittivity in vacuum ε_0 times the

relative dielectric permittivity ε_r for the specific medium. The relative dielectric permittivity, or simply relative permittivity, is also known as the dielectric constant.

The second term in eq. (16) describes the dampening of wave energy due to ohmic losses, transformation from electric or magnetic energy into heat. The impulse wave amplitude decays then with distance in the following way:

$$\boldsymbol{E} = \boldsymbol{E_0}\, e^{-\beta z} = \boldsymbol{E_0}\, e^{-\frac{\sigma \mu v}{2} z} \tag{19}$$

where $\boldsymbol{E_0}$ is the radiated energy level.

In additional to the ohmic energy losses, the wave amplitude also suffers geometric attenuation losses with distance, as the energy spreads in space from a point source. This energy decay can be estimated by using the radar range equation if the distance between the receiver and transmitter are greater than some wavelengths (Annan, 2003). To make more precise determinations of those losses care has to be taken about the antenna type used and objects interacting with the electromagnetic field among others. If measurements are performed with the same antenna separation every time the geometric energy losses can be disregarded, further considered in section 2.2.3.

2.1.3. Propagation paths of impulse waves

The travel paths of the wave must be considered in order to determine the volume actually affecting each measurement. Two different models were used concerning the spreading of the electromagnetic wave: ray-theory assuming straight travel paths, and the Fresnel volume concept assuming a certain influence area around the direct path.

By using so-called ray theory, the electromagnetic wave can be characterized as propagating through space on a narrow line joining the transmitter and receiver. Strictly, this is only possible by assuming that the wave has an infinite frequency (Spetzler & Snieder, 2004)., The material properties that can be derived from the impulse wave represents an average along the direct path between the transmitter and receiver antenna with this approach.

On the other hand, when using low frequencies the direct ray approximation becomes more invalid. In reality, the velocity and attenuation of the impulse wave are affected by a volume surrounding the direct travel path. The volume affecting the wave travel properties is defined as the Fresnel volume (Johnson *et al*., 2005) characterized by a maximum diameter *l* and a distance *d* (Figure 2). With this approach, the traveling medium properties determined from the velocity and attenuation of the electromagnetic impulse wave are assumed to represent average values of the material properties within the Fresnel volume.

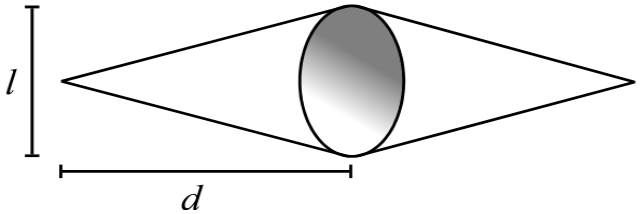

Figure 2. *Fresnel volume with diameter l and distance d from source to middle. The gray marked area is referred to as the Fresnel zone.*

An expression for the diameter *l* of the Fresnel zone, defined as any cross-section on the Fresnel volume, can be stated as a function depending on the electromagnetic wave frequency *f* and the

distance d from the transmitting or receiving antenna (Annan, 2003). When d equals half the distance between the antennas the diameter l is the greatest diameter on the Fresnel volume.

$$l = \sqrt{\frac{d\ c}{2\ f}} \tag{20}$$

The Fresnel volume can be approximated by the volume of two equal cones with height d and diameter l (Annan, 2003).

$$V_f = \frac{\pi}{12}\ \frac{d^2 c}{f} \tag{21}$$

The ray theory and the Fresnel volume concept considered above are simplified models of reality. For a complete wave propagation description care has to be taken on which antenna type is used for example.

2.2. Theory applied on canopy measurements

The theoretic approach for the spreading of an electromagnetic impulse wave described in section 2.1 is often used when evaluating GPR surveys. The assumptions used for the theoretical results can also be considered valid for impulse radar transmission measurement through forest canopies:

- Only very small amounts of free charges exist in the canopy air space.
- The low loss criteria can be used as the dielectric permittivity and conductivity of the canopy and an eventual interception storage are small compared to the angular frequency of the impulse wave generated by the GPR antenna.
- The medium can be assumed to be homogeneous and isotropic when using wavelengths greater than single components of its constituents (Sihvola, 1999).
- Ferromagnetic materials are not present in the canopy air space.
- A few wave lengths away from the transmitting antenna the impulse wave propagates on a plane perpendicular to the traveling direction (Annan, 2003).
- Small constant changes of the electromagnetic properties for the canopy and an eventual interception storage within the used frequency region (Annan, 2003; Fletcher, 1970).

2.2.1. Electromagnetic mixing formulas

The dielectric constant of a medium can be described as its capacity to store electric energy and can, as already shown, be estimated from the velocity of an electromagnetic impulse wave. Dielectric constants of single element solids and liquids such as water and ice are rather well known. However, in most practical applications the relative permittivity of mixed materials such as soil or snow is more interesting. The correlation of the dielectric constant to other material characteristics, such as the volumetric content of its constituents, are known as so-called dielectric mixing formulas (Sihvola, 1999).

The ability to use such medium descriptions depend on one important physical aspect of electromagnetic waves. Objects smaller than the wave length can not be resolved as one single unit, but it does not imply that the electromagnetic wave is unaffected by them. The interpretation of this

is that small objects effect the wave as if it were traveling through an isotropic homogeneous medium with some average electromagnetic properties (Sihvola, 1999). Therefore, by choosing an appropriate wavelength for the interception measurements the canopies and snow stored on them can be considered as an isotropic homogeneous medium (Angot *et al*., 2002). During this work only antenna frequencies giving a wave length above around four decimeters have been used. No single components of the trees studied greatly exceeded this boundary.

One example of a mixing formula preferred by many authors for correlating the dielectric constant to water content is Lichtenecker's equation (22) (Zakri *et al*., 1998). Lichtenecker used the volumetric content of the material constituents θ_c, where water is one of these fractions, and their dielectric constants ε_c to describe the relative permittivity ε_m of the medium.

$$\varepsilon_m = \left(\sum \theta_c \varepsilon_c^{\alpha} \right)^{1/\alpha} \tag{22}$$

One appropriate method to estimate the density of snow and its water content is to determine its relative dielectric properties at radio frequencies. Frolov (1999) used experimental data to find approximations appropriate for practical purposes. The main snow components are air, ice and water. All have constant dielectric properties in the studied frequency region from 1 MHz to 10 GHz. Structure dependent descriptions were omitted, though they were considered useless for practical reasons. One special case of Lichtenecker's equation considered by Frolov (1999) was when $\alpha = 1/3$. This is know as Looyenga's formula. Frolov showed and concluded that experimental data by other research groups for dry and wet snow was well enough reflected on average by that equation. In this study a variant of Looyenga's mixing formula was derived to fit the situation of an interception storage in the forest canopies from eq. (22):

$$\varepsilon = (\theta_{air} \varepsilon_{air}^{1/3} + \theta_{tree} \varepsilon_{tree}^{1/3} + \theta_{water} \varepsilon_{water}^{1/3} + \theta_{ice} \varepsilon_{ice}^{1/3})^3 \tag{23}$$

which can be further simplified as the dielectric constant of air is approximately one:

$$\varepsilon = (\theta_{air} + \theta_{tree} \varepsilon_{tree}^{1/3} + \theta_{water} \varepsilon_{water}^{1/3} + \theta_{ice} \varepsilon_{ice}^{1/3})^3 \tag{24}$$

Applying dielectric mixing formulas to a forest environment isn't well studied but would, according to Sihvola (1999), have good conditions to be valid for dense canopies.

For conductivity straight-forward mixing formulas does not exist in the same extension as for the dielectric constant. Motion of free electric charges in a medium induced by electromagnetic waves are determined by its conductivity. This property depend among others on the structure of the matter deciding the travel paths of the free charges. For snow the shapes of the individual ice crystals and their mutual alignment therefor strongly influence the conductivity. The structure dependence of biological matter, as the tree cellulose, is also hard to identify. Mixing formulas for conductivity suitable for practical use to this study have not been found during the literature studies. Archie's law, often used to relate conductivity to water content in soils, was considered to have some potential for this study (Annan, 2003). However, as this equation contains several calibration parameters it was unsuited for evaluation during the relative few and short measurements performed. Amplitudes and conductivities will be treated further on as well, in spite of missing mixing formulas, as they are considered to be interesting parameters, and maybe giving useful information.

2.2.2. Radar equipment

For this study, a ground penetrating radar system RAMAC/GPR from Malå Geoscience AB, Sweden, was used. The radar has a high travel time accuracy, is designed for field conditions and is easy to use. However, applying this technique to determine the extremely small travel time and attenuation differences that may arise as a function of snow interception requires a good understanding about the system performance. The most critical factor to take into consideration is drifts in system components which affects the travel time determination.

The system consists of a transmitting and a receiving antenna, each connected to a control unit via fiber optical cables. Instructions on how a measurement series is controlled is given from a computer to the control unit (Figure 3). When starting a measurement, a trigging signal is sent from the control unit to both antennas and a time mark is made. An impulse wave is generated by the sender antenna and is detected by the receiver antenna after transmission through the medium in between. Detected amplitude values at the receiving antenna are sent back to the control unit where the time for the whole process is determined. In a sampling radar system, the digital converter in the receiving antenna can not capture sufficient number of points on the whole impulse wave in one single measurement. Instead the transmitting-receiving procedure is repeated with a slight time delay on the receiver antenna compared to the previous measurement. Only one wave amplitude value is detected by the receiving antenna at a time. This procedure is repeated until a desired number of samples on the impulse wave is determined. The *sampling frequency* equals the number of sampling points per second. The inverse of the sampling frequency times the number of measured points used to capture the wave gives the total measured time interval, which is called the *time window*. In order to detect a certain travel time change, the time window must be larger than the greatest variation in time. The change in travel time depends on both the antenna separation and the expected variation of dielectric constant within the traveling medium, in our case the forest canopies.

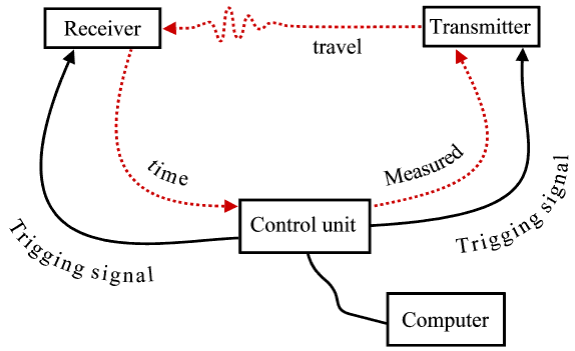

Figure 3. *The radar system consists of a control unit connected to a transmitting and a receiving antenna. The control unit is controlled by a computer.*

Three different antenna types were used during the tests performed in this study: 200 MHz unshielded antennas, and shielded 500 and 800 MHz antennas. The unshielded antennas gives spreading of the generated electromagnetic wave in all directions, while in a shielded antenna the electromagnetic impulse wave is only allowed spreading in one direction and disturbances from other sources are reduced.

2.2.3. Evaluation of dielectric constant and conductivity

This section describes the procedure to determine dielectric constants and conductivities from radar measurements of travel times and amplitudes.

A single measurement of an impulse wave can be shown in an amplitude versus time graph

as a so-called trace (Figure 4). For every measured impulse wave a first arrival in travel time has been determined from this pulse. The greatest positive single peak has been interpreted as the first arrival of the impulse wave, where the corresponding time and amplitude are given by the sample number.

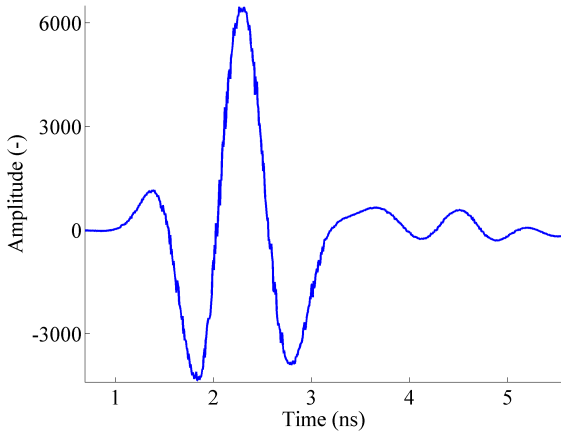

Figure 4. *A measured impulse wave represented as a so-called trace in an amplitude versus time plot. The highest positive peak is interpreted as the first arrival time of the pulse.*

A series of measured traces captured as the antennas are moved along a measurement line are often represented by a so-called radargram, where all measured traces are plotted beside one another (Figure 5). In this case, each trace is identified by the distance the antennas were moved. The amplitudes are represented by a gray scale. From the presented radargram one can observe a slight change in arrival time for the amplitudes over the measured distance interval.

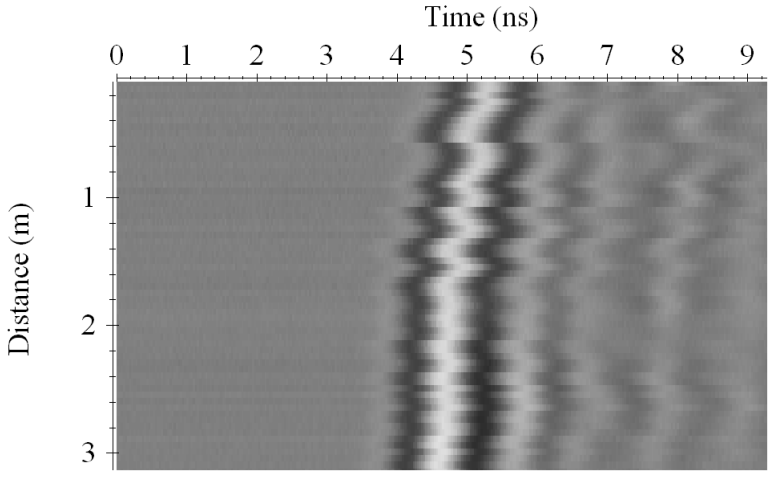

Figure 5. *Example of a radargram. Bright areas represent positive amplitudes on the impulse wave and dark regions represent negative amplitudes. Single traces are identified by a distance.*

The first arrival time determined from a trace is not necessarily equal to the absolute travel time of the impulse wave, due to unknown time losses in the fiber optical cables and the electronics of the radar system. These losses can be estimated by performing a reference measurement in air t_r for a given antenna distance l. The time to correct the first arrival is calculated as the difference between the reference measurement t_r and the true travel time in air t_t assuming the speed of light. The impulse wave speed v can then be estimated from the travel time of a measurement t_m with eq. (25):

$$v = \frac{l}{t_m + t_t - t_r} \tag{25}$$

By rearranging eq. (18) into eq. (26) the relative permittivity ε_r can be determined from the estimated velocity:

$$\varepsilon_r = \left(\frac{c}{v}\right)^2 \tag{26}$$

The ohmic dissipation in air can be assumed to be zero, as no electromagnetic conduction exists there. This means that the exponential attenuation term in eq. (19) equals unity. Only geometrical energy losses are apparent due to the spreading of energy in space, described by a function $f_r(l)$, where l is the distance between the antennas (Annan, 2003). These energy losses are hard to estimate since they depend on the type of transmitting antenna, the distance to the ground, and other objects affecting the electromagnetic field etc. The type of receiving antenna also influence the measured amplitudes, which is described by the function $f_a(l)$ (Annan, 2003). For the reference measurement in air, the amplitude $\boldsymbol{E_r}$ detected by the receiving antenna can be estimated with the following equation.

$$\boldsymbol{E_r} = \boldsymbol{E_0}\, f_a(l)\, f_r(l) \tag{27}$$

For all other measurements the detected amplitudes $\boldsymbol{E}$ can be estimated by combining eq. (19) with the same functions describing the geometric energy losses $f_r(l)$ and a the energy captured by the receiving antenna $f_a(l)$ used in eq. (27).

$$\boldsymbol{E} = \boldsymbol{E_0}\, e^{-\beta l}\, f_a(l)\, f_r(l) \tag{28}$$

Dividing eq. (28) with eq. (27) gives the attenuation factor β:

$$\beta = \frac{1}{l} \ln \frac{\boldsymbol{E_r}}{\boldsymbol{E}} \tag{29}$$

The conductivity σ is then given by combining eq. (15) with eq. (29) and is a function of measured amplitudes, the impulse wave velocity and the antenna separation:

$$\sigma = 2\,\beta\sqrt{\varepsilon} = \frac{2}{v\,l} \ln \frac{\boldsymbol{E_r}}{\boldsymbol{E}} \tag{30}$$

where the magnetic susceptibility μ is assumed to be equal to unity.

2.2.4. Signal processing

A Matlab program was designed to achieve the best possible determination of the first arrival time.

The detected raw signal may contain high frequency noise. The noise can be reduced with a third order low pass digital Butterworth filter (Mathworks, 2006). This type of filter is maximally flat in the frequency passband which makes a minimum alteration on the wanted signal. However,

the filtering causes a slight frequency dependent time-delay of the processed signal compared to the raw signal. As the frequency content of every individual measured traces is assumed to be equal this time-delay is in the same magnitude for every processed signal, and the estimated velocities using eq. (25) remain unaffected.

To increase the accuracy of the detection of the first arrival times, in other words the time of the maximum amplitude, spline functions were interpolated to the filtered measured values. A spline is defined as a function determined piecewise by polynomials which intersect one another at knots, having the same value and first derivate there (Råde & Westergren, 1998). After these two signal processing steps the top of the highest pulse from the example trace above gets the appearance depicted in Figure 6.

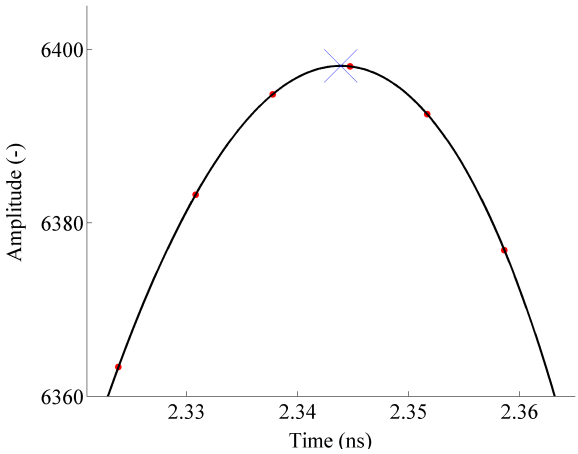

Figure 6. *The highest peak of the first arriving pulse from one trace. Points represent noise reduced measured samples. The curve shows the spline interpolated from these values. From the highest amplitude of the spline, represented with a cross, the pulse arrival time is determined.*

The impulse wave travel time and amplitude was picked from the interpolated curve. These values were used to estimate wave velocity and attenuation. The accuracy of these values depend on both the choice of antenna and sampling frequency. By using a high antenna frequency the peaks get more marked and specific maximum values are easier to pick. The sampling frequency is to be set high to achieve good accuracy. However, the time window decreases as the sampling frequency is increased. A compromise has to be done between the accuracy and the measured time interval.

2.2.5. Translation of impulse wave velocities into interception storage

As discussed above, the dielectric constant of the canopy air space can be determined with eq. (26) from the impulse wave velocity. The dielectric constant of the canopy air space can be related to the components of air, tree material and water or snow with Looyenga's formula, eq. (24). Considering the changes of the tree fraction as small, then the variations of air, ice and water fraction in relation to a reference measurement can be determined with the following difference derived from eq. (24):

$$\varepsilon_m^{1/3} - \varepsilon_r^{1/3} = \Delta\theta_{air} + \Delta\theta_{ice}\,\varepsilon_{ice}^{1/3} + \Delta\theta_{water}\,\varepsilon_{water}^{1/3} \qquad (31)$$

where ε_m and ε_r represents the dielectric constant of the measurement and of the reference performed.

The ice and water contents of the intercepted water are unknown, and therefore it is assumed that either only ice is present at temperatures below 0°C and only water is present at higher

temperatures. The volumetric fraction of intercepted water in the canopy air space is further on referred to as the interception fraction θ_i. As the air volume decrease is equal to the increase of interception fraction, a change in the interception fraction between two measurements can be determined with the following equation:

$$\Delta\theta_i = \frac{\varepsilon_m^{\frac{1}{3}} - \varepsilon_r^{\frac{1}{3}}}{\varepsilon_i^{\frac{1}{3}} - 1} = \frac{\left(\frac{c}{v_m}\right)^{\frac{2}{3}} - \left(\frac{c}{v_r}\right)^{\frac{2}{3}}}{\varepsilon_i^{\frac{1}{3}} - 1} \tag{32}$$

where ε_i represents the relative dielectric permittivity of ice or water, and v_m and v_r represent the measurement and the reference velocity, respectively. The actual amount of ice or water can be determined if an estimation of the actual measured volume is available.

2.3. Laboratory tests

2.3.1. Experimental procedures

The site for these experiments was Malå. Most tests were performed in an indoor hall, where conditions such as air temperature and moisture were relative constant. The basic installation for most of the experiments was with two antennas pointing at each other with a small tree in-between (Figure 7). The small tree was lifted up and down with a lifting device, measurements starting with the lower end of the tree near the ground. For every centimeter the tree was raised a new measurement was taken, one single trace captured. Both antennas were placed in fixed positions at 2.0 m elevation and separated by a distance of 2.5 m. The tree used during the tests was a ~2.7 m tall Norway spruce. Every single profile measurement of the tree ended with an air reference measurement which were used both to correct for time depending drifts and to determine the impulse wave velocities from the measured travel times using eq. (25). Interception on the tree was for practical reasons created by watering with a watering can, instead of using snow. The greater impact of water on the electromagnetic field properties was believed to compensate for the lower interception capacity compared to snow. An independent measure of the interception storage was made with a scale attached to the top of the tree.

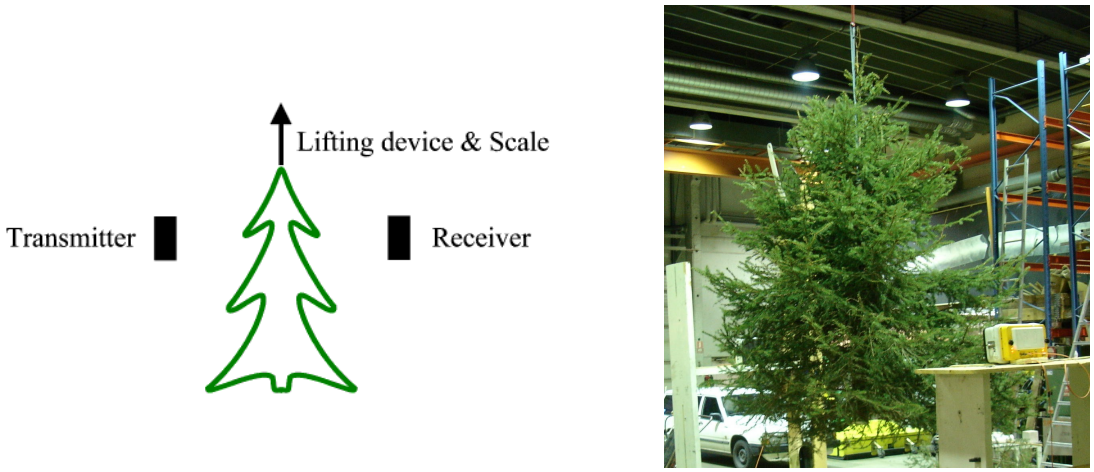

Figure 7. *Schematic illustration (left panel) and a photograph (right panel) of the basic setup for the single tree profile measurements in Malå.*

To avoid the influence of metal objects the antennas were placed on wooden constructions. Cables

connecting the antennas and the control unit were fixed to prevent movements during the measurements. By these steps other factors influencing the measurement were believed to be minimized.

2.3.2. Drifts

It is important to know the gradual change of output due to instrument drifts, especially in the case of measurements in canopies when the variation of the dielectric properties are small. Measurement drifts can depend on several factors, such as instrument imperfections and temperature variations.

Radar equipment normally needs some time to warm up when switched on before measured values stabilize. The behavior of the antennas during warm up was observed by making continuous measurements for twenty minutes with only air between the antennas.

Drifts can also occur when the fiber optical cables between the antennas and the control unit are moved or bended. During a second test measurement the cables were moved randomly to quantify this disturbance. The connections from antenna or control unit to the fiber optical cables were also dislodged.

2.3.3. Antenna frequency and sampling frequency

A series of vertical profile measurements on the tree in dry condition was performed for every type of antenna only varying the sampling frequency. From the results an appropriate value on this parameter was chosen for the specific antenna frequency and the actual measurement setup.

Secondly, the tree was wetted step-wise with 2-5 liters of water. Immediately upon wetting the tree, a new radar profile measurement was made. The weight of the wetted tree was observed before and after each radar measurement. After letting the tree dry this procedure was repeated for the different antennas. The mass of the interception storage was calculated as the difference between the weight of the tree in wet and dry conditions.

In addition to the test of antenna and sampling frequency, these profile measurements were used to make an empirical estimate of the maximum diameter of the Fresnel volume as a comparison with the theoretical, eq. (20). The zone affecting the impulse wave was detected as the bottom of the tree was passing the level of the antennas.

2.3.4. Experimental evaluation of mixing formulas

Two different experiment set-ups were used to test the applicability of Looyenga's formula to model the dielectric constant of a vegetation canopy with rain interception.

First, the velocities estimated from the single tree profile measurements described above were translated into volumetric water contents at every level, for each trace, with eq. (32). The results from the measurements with the dry tree was used as reference. By assuming ray theory to be accurate, the estimated water content of each trace θ_z could be considered to represent the average water content of a horizontal plane in the tree. The amount of water per square meter (kg/m^2) in vertical layers, with thickness Δz of 1 cm, was further estimated by multiplying the water contents from each trace with an horizontal unit area A and the distance between the adjacent measured points on the profile (1 cm). The density of water is set to 1 kg/litre. Summing all estimated water amounts over the profile gave a total amount of water I per square meter intercepted in the tree:

$$I = \sum \theta_z \, A \, \Delta z \qquad (33)$$

Finally, the interception storage estimated from the radar measurements was multiplied with the lower area occupied by the tree (approximately radius of 1.25m gave the area 4.9 m^2), in order to be comparable with the tree scale measurements. Of course the distribution of the tree mass and the intercepted water was not perfectly homogeneous. However, this assumption was necessary to make if the two measurements are to be compared quantitatively.

For the second experiment the basic installation was rearranged. The antennas, 800 MHz shielded, were lowered to 1.0 m above the ground and separated by a distance of only 1.25 m. Cut-off spruce branches were hung under a square wooden construction attached to the lifting device and the scale (Figure 8). The hanging branches were assumed to be a completely homogeneous test sample, forming a dense cube with sides of approximately 1.0 m. By weighing the branches and the device an independent value for the amount of water pored on the branches was calculated.

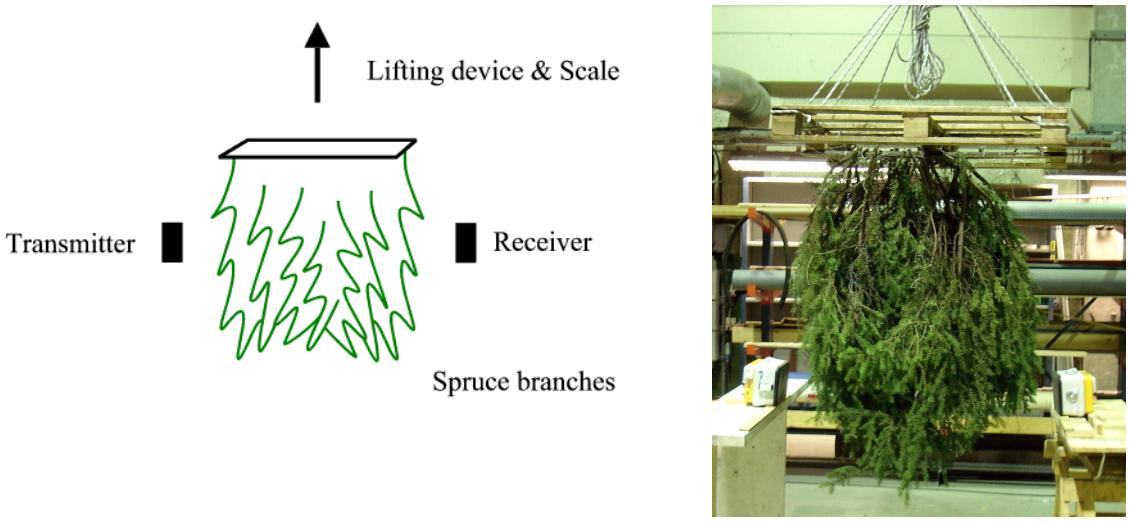

Figure 8. *Compact hanging spruce branches were attached to a lifting device and a scale and placed between the radar antennas. Schematic illustration (left panel) and photograph (right panel).*

The radar measurements were trigged manually at specific times and were conducted with the branches always hanging in the same position. Air reference measurements were performed at evenly distributed occasions and used to correct for instrument drifts. The branch bunch was elevated well above the level of the antennas before the air reference measurements, and lowered again to the same position before next interception measurement.

Impulse wave velocities and volumetric water fractions were estimated as previously described based on the measured travel times using eqs. (25) and (32). The first measurements without any intercepted water on the branch bunch was used as reference for the derivation of the intercepted water amounts.

For this experiment, the comparison of the radar measurements and scale measurements was based on the Fresnel volume concept. A volume of 38.4 liters influencing the radar measurements was estimated using eq. (21) with antenna separation 1.25m and frequency 800 MHz. This volume times the estimated water fraction was used as an estimate of the amount of water on the branches. The weighted values of water were scaled with the ratio of the Fresnel volume and the total volume occupied by the branches. The latter was estimated assuming that the branch bunch was a cube with 1 m sides.

2.3.5. Attenuation with distance

The amplitude extinction due to increasing antenna separations was tested in a relatively dense and homogeneous forest outside Malå. This is an important factor to take into account for the design of a field scale instrumentation. It is desirable to maximize the antenna separation in order to get the most representative measurement. On the contrary, it is important to get a reasonable high amplitude-to-noise ratio in the signal to be able to identify the first arrival accurately.

The receiving antenna was placed in a fix position 3.0 m above ground level and the transmitting antenna, elevated approximately 2.5 m, was moved in two meter steps away from it, starting with a separation of one meter, and ended with an antenna separation of 25m. At each stop, measurements were trigged manually. The procedure was carried through for the 200 and 800 MHz antennas. The ratio of the first arrival amplitudes and the average amplitude of the tail of the trace at 5 m antenna separation were used to determine the amplitude-to-noise ratio. The trace at 5 m distance was used to estimate the amplitude of the noise, since it had a well defined impulse wave within the first third of the samples.

2.3.6. Accuracy and uncertainty estimations

A simple approach to estimate accuracy and uncertainty of the measured impulse wave velocities and amounts of water is presented in this section. The accuracy of the time determination process of the first arriving pulse is assumed to be the inverse of the sampling frequency, which is equal to the time difference between two adjacent sampling points on the trace. The maximum uncertainty of the estimated travel time of the impulse wave was taken equal to the accuracy, which should be a fair guess if the selected data point is the one nearest the true peak. With a known antenna separation l the uncertainty in the velocity estimate Δv can be derived by comparing the time for two adjacent sampling points on the trace, t_i respectively t_{i+1}:

$$\Delta v = \frac{l}{t_i} - \frac{l}{t_{i+1}} \tag{34}$$

As the uncertainty of wave velocity is a function of the travel time, or its own speed, the estimations are presented as in Figure 9. Assuming that Looyenga's mixing formula is valid, the uncertainty in fractions of water is estimated with eq. (32) using the uncertainty of the impulse wave speed. The velocity span showed is greater than highest expected wave speed decrease due to raised snow or water content.

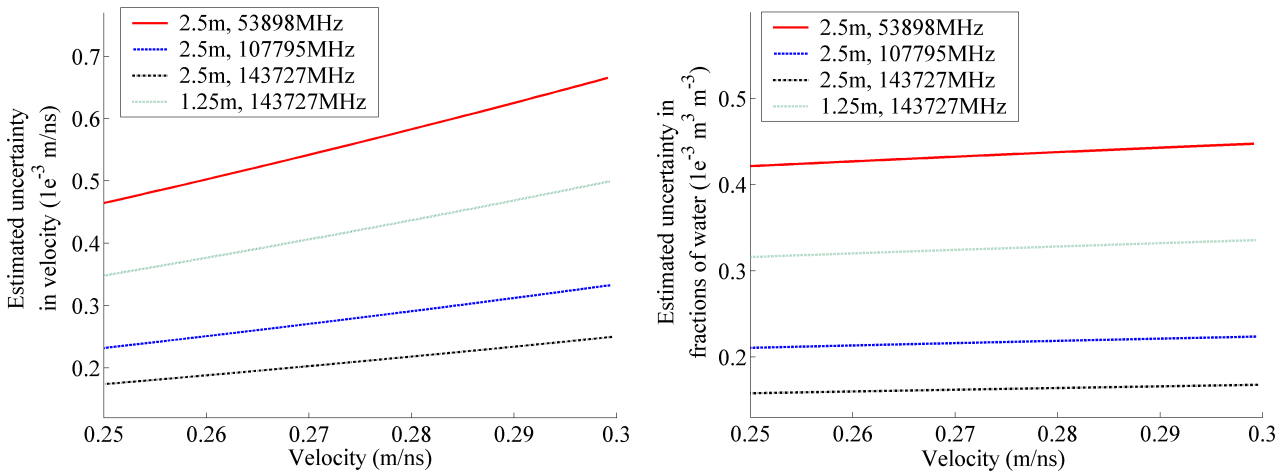

Figure 9. *Estimated uncertainties for the impulse wave velocities (left panel) and changes in water fractions (right panel) as a function of the pulse speed for some sampling frequencies and at different antenna separations.*

To estimate the uncertainty for the amounts of water determined during the single tree profile measurements the mean uncertainty in water fraction over the velocity range 0.25-0.3 m/ns for the specific antenna separation 2.5 m and sampling frequency 143727 MHz was derived. This value times an horizontal unity area, the distance between the adjacent measured points on the profile and the number of measured levels, eq. (33), gave an uncertainty of 0.37 kg/m^2. By multiplying this with the ground area occupied by the tree (4.9 m^2) the uncertainty of the total amount of water on the tree became 1.8 kg.

To estimate the uncertainty of the amounts of water derived from the experiment using hanging spruce branches the mean uncertainty in water fraction calculated over the velocity range 0.25-0.3 m/ns was multiplied with the Fresnel volume (38.4 liters). The highest estimated uncertainty in amount water was thus $12.5 \cdot 10^{-3}$ kg.

2.4. Field experiments

2.4.1. Study site

The field scale measurements were performed in the Flakaliden Research Park (N E coord, ~300 m.a.s.l.) run by the Swedish University of Agricultural Sciences, located about fifty kilometers east of Umeå. This site was considered to be appropriate for the measurements for several reasons. First of all, the weather conditions are favorable, the chances of snow fall are likely. The vicinity to the sea can cause fast changing temperatures leading to high evaporation courses. In other words, the chances of a varying snow storage on the trees during the measurement series were considered as good. The forest at Flakaliden is a dense relative young spruce stand and the tallest trees are around six to seven meters high.

2.4.2. Measurement setup

Two masts, the lowest reaching just above the highest trees, separated by a distance of 13.5 m were used for the measurements. One pulley was attached to the top of each mast and two others to the lower end. A wire used to rise and lower the antennas was driven and guided by this pulley system (Figure 10). With this approach the antennas were at the same elevation during the vertical profile measurements.

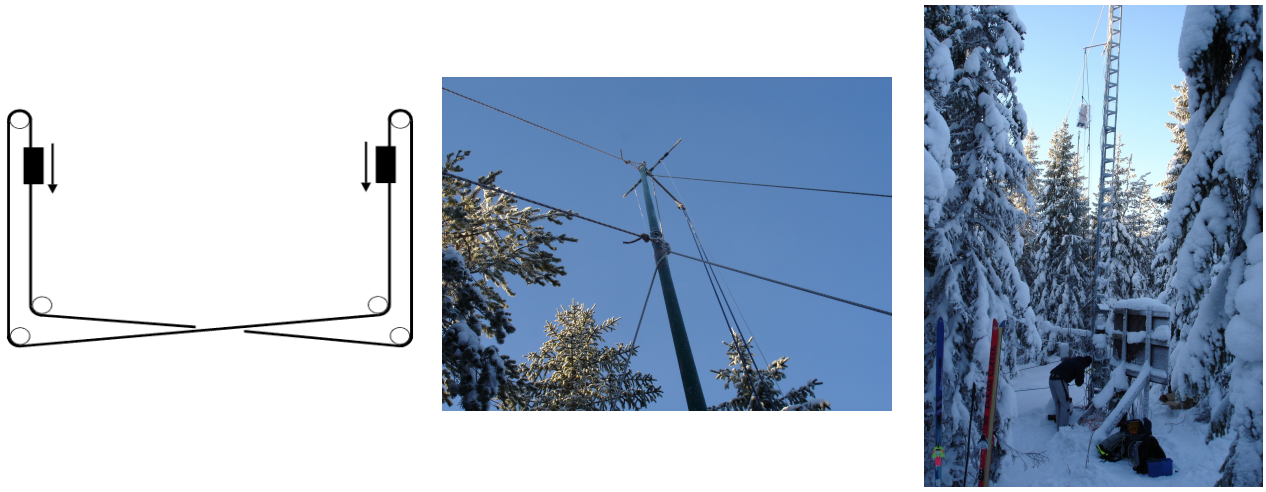

Figure 10. *Schematic illustration of the wire and pulley system used to move the antennas (left panel) and photographs of the masts (middle and right panel).*

The antennas were raised and lowered by hand. To minimize horizontal dislocations of the antennas they were fixed at two wires running along the masts. The 800 MHz antenna was used for these measurements due to its better spatial resolution and higher travel time accuracy compared to the lower frequency antennas. Fiber optical cables with reinforced lining compared to the ones used during the laboratory tests were chosen to prevent drifts due to cable movements and bending. The connections between antennas and cables were fixed in locked positions. Every single measurement was started with the antennas raised to the top position and slowly lowered. At every fifth centimeter a new point measurement was trigged and the first measured points on the profile served as air reference.

2.4.3. Measurements

Drifts due to cable movements and dislodgement of the connections at the antennas were measured during one first test, holding all other influences constant.

Over four days and at four different occasions several measurement series were captured. On evening January 18 the first measurement was performed. During the night between the 18 and 19 January, white frost had been formed on the trees. To capture this change and an eventual evaporation, measurements were performed both at midday and at the evening of January 19. A minor snowfall occurred before the last measurement on January 21. Due to low temperatures over the period, around -20ºC, the intercepted snow was assumed to be free from liquid water. From the profile measurements velocities were estimated using eq. (25). With eq. (32) the results were translated into fractions of ice at every level using the velocity results from the first measurement as reference. A change in interception storage (kg/m^2) with respect to the reference measurement was achieved by using eq. (33) and scaling with the quot between the density of ice and water.

On evening January 20 the tree weighing device for intercepted snow, earlier used by Lundberg (1993), was installed in order to achieve an independent measurement value of snow interception changes. A cut spruce was placed and fixed on an automatic recording balance,

delivering weights every half an hour. A plastic sheet covering but not touching the scale prevented throughfall of snow disturbing the measurement. The weight of the bare tree was used as reference value to derive changes of the snow interception storage on the tree. The measured snow mass on the tree was divided by the ground area occupied by the spruce (approximately radius of 0.5 m gave the area 0.8 m^2) to achieve an amount of water per square meter comparable to the radar measurements. Trees covered by the radar measurements were a couple of meters taller than the tree on the scale why this value was raised by a factor 1.4. A rescaling factor for the snow mass intercepted by the tree to a forest stand was not available. Simply, it was assumed that there is one tree of this widths but seven meters tall per square meter in the forest.

During one last measurement series snow was shaken of the trees between single performed measurements. As above, velocities and fractions of ice with respect to the first measurement were estimated.

2.4.4. Accuracy and uncertainty estimations

The uncertainty analysis in this section follows the same approach presented in section 2.3.6, only for the antenna separation and sampling frequencies used during these field measurements (Figure 11).

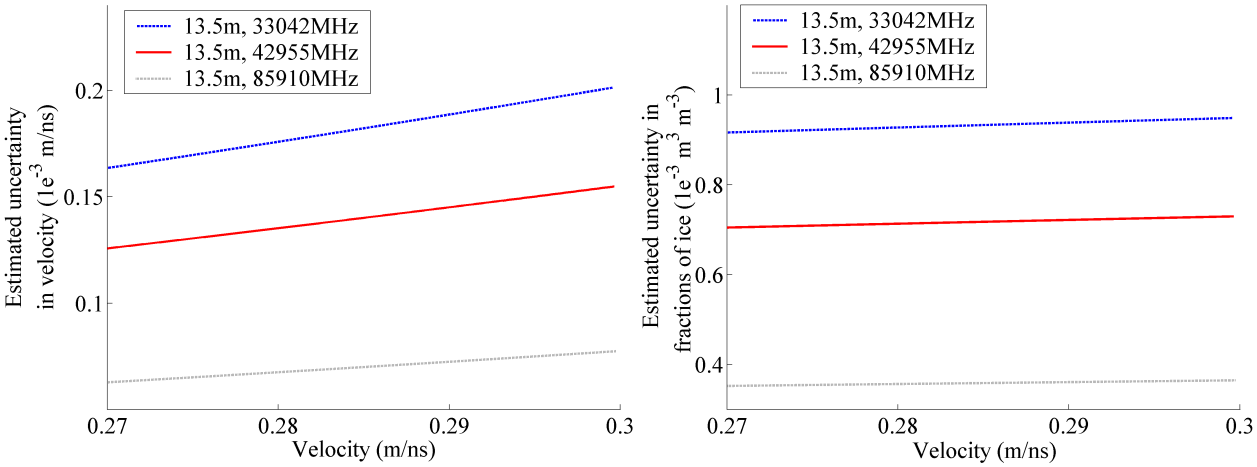

Figure 11. *Estimated uncertainties for the impulse wave velocities (left panel) and changes in water fractions (rigth panel) as a function of the pulse speed for used sampling frequencies.*

For the lowest and the highest sampling frequencies presented here the uncertainty in interception storage of water are estimated to 3.9 kg/m^2 respectively 1.5 kg/m^2, using the quot between the density of ice and water.

The antennas could move about 0.02 m horizontally and 0.1 m vertically each during the transmission measurements, movements influencing the results. For the estimations of the impulse wave velocities with eq. (25) a difference from the used distance (13.5m) of the antenna separation to the true distance of approximately 0.042 m could occur. With eq. (34) the difference in distance can be translated into a highest uncertainty in velocity of $0.92 \cdot 10^{-3}$ m/ns, comparing with the travel time of light. Using eq. (32) the highest uncertainty in fractions of ice is $4.3 \cdot 10^{-3}$ $m^3 m^{-3}$ and amount of water per unit area for the profile becomes 18.4 mm/m^2 with eq. (33) and using the quot between the density of ice and water.

3. Results

3.1. Laboratory tests

3.1.1. Drifts

Large travel time disturbances were measured during the warm-up period of the radar equipment. These variations, in the magnitude of nanoseconds, seemed to behave in some sense randomly. After the initial phase lasting a couple of minutes a more moderate drift occurred rising the travel time with approximately 0.020 ns/min. These drifts were captured during a measurement lasting twenty minutes.

Movements and bending of the cables resulted in sharp leaps in the travel time measurements. The greatest travel time differences observed were around 0.15 ns. The measured amplitude was not effected at all as the cables were moved. First when pulling the connections between the antennas and the cables this value started to vary. The travel time was also effected by these actions. Leaps of around 0.2 ns were measured.

3.1.2. Antenna frequency and sampling frequency

Values measured beneath one nanosecond on every trace represents a zero level amplitude before the first pulse is detected (Figure 12). The arrival times are interpreted from this pulse. The travel time slowly increases from the top of the tree at 0 m to near the lower end of the tree at ~1.5 m. At profile positions above ~1.5 m the travel time relative rapidly decrease until only air is measured at about 2.0 m, which was well below the bottom of the tree as it was lifted upwards through the antenna beam. The high sampling frequency used to achieve better accuracy resulted in a narrow time window. Reflected waves from surrounding objects and waves traveling more time consuming ways around the tree can not be observed in the radargram.

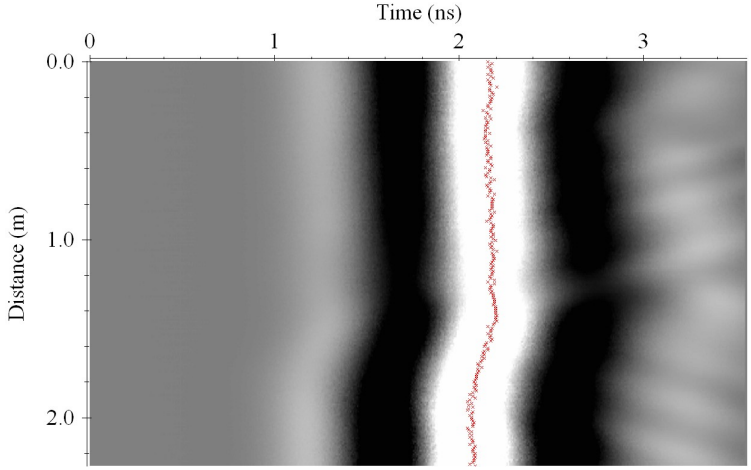

Figure 12. *Radargram from a single tree profile measurement, from the top of the tree (0 m) to its lower end (~1.7 m), using an 800 MHz antenna. Bright areas represent positive amplitudes on the impulse wave and dark regions represent negative amplitudes. The first arrival times interpreted for the impulse waves are marked with crosses.*

From the first arrival times marked with crosses in the radargram (Figure 12), velocities were estimated. These are presented along two further profile measurements of the single spruce after being wetted (Figure 13). At positions above 2.0 m only air was affecting the impulse wave. The 0.5 m wide zone just above the air reference shows a steady decrease in velocity. This is interpreted

as the zone on which the electromagnetic field inhibited influence. As the tree was wetted the first time, the velocities decreased more at the top of the tree than the lower end. A slight change in form of the curve can be observed. As the amount of water was raised in a final step an additional impulse wave speed decrease was estimated. The changes are greater at the lower end of the spruce compared to the first wetting occasion. Both these curves have the same form. Using the profile measurement of the dry tree as reference, changes in water fraction was estimated from the velocities at every level. At the first wetting occasion a greater change near the top of the spruce can be observed. The final measurement shows a greater increase in amount of water at the lower end of the tree.

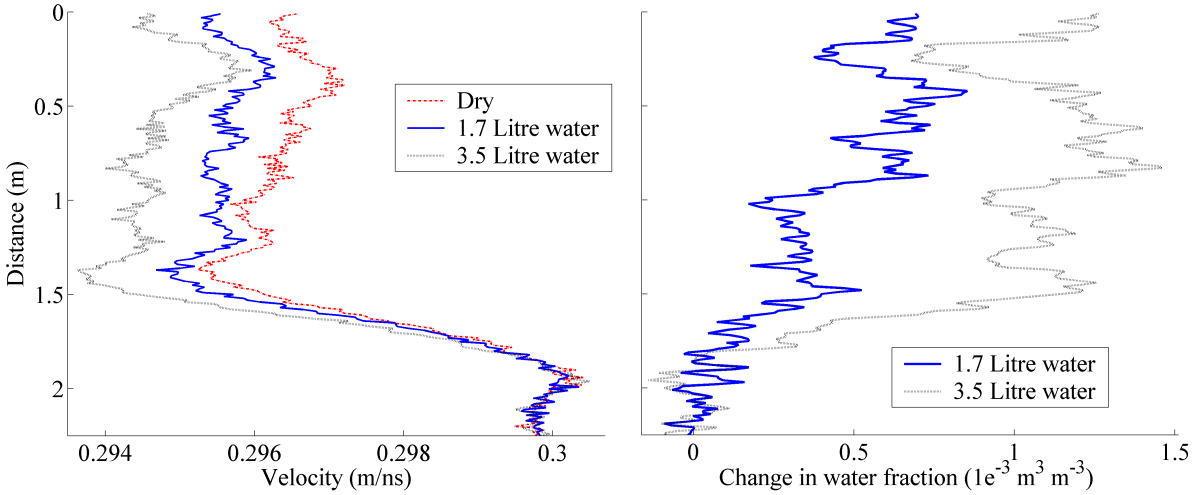

Figure 13. *Impulse wave velocities (left panel) and changes in water fraction (right panel), derived from single tree profile measurements, from the top of the tree (0 m) to its lower end (~1.7 m), with different amounts of water on the tree, using an 800 MHz shielded antenna at a sampling frequency of 143727 MHz. Changes in water fraction estimated from the presented velocities.*

For the 500 MHz shielded antenna a result similar to that captured with the 800 MHz antenna was observed. A slight lower velocity decrease, around $3 \cdot 10^{-3}$ m/ns, for the dry tree was determined. The velocity decrease due to the water pored on the spruce was both in the same weight increase as in velocity decrease as for the 800 MHz antenna.

The use of a 200 MHz unshielded antenna for the single tree profile measurements gave a complete different result compared to the higher frequency measurements (Figure 14). From the lower end of the spruce, distance ~1.7 m, to the top of it, distance 0 m, a similar decrease for the impulse wave speed was determined for all levels of interception storage. No velocity changes due to raised water amounts were detected. Furthermore, the shape of the measurement profiles indicate a completely different influence area compared to the higher frequencies. The 1.0 m wide zone above the air reference measurement with the velocity steady decreasing was interpreted as the influence zone of the impulse wave.

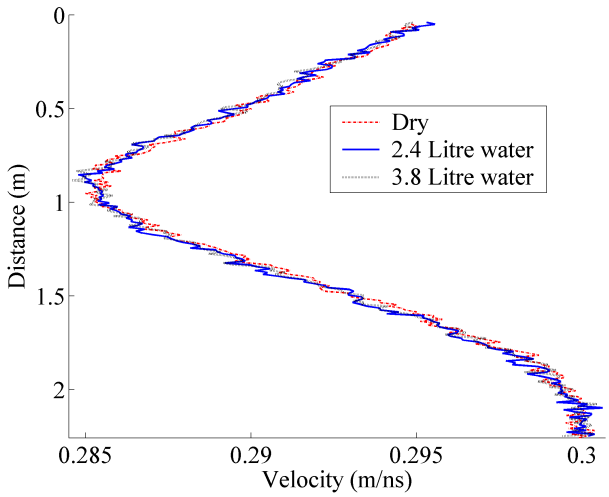

Figure 14. *Impulse wave velocities derived from single tree profile measurements, from the top of the tree (0 m) to its lower end (~1.7 m), with different amounts of water on the tree, using an 200 MHz unshielded antenna at a sampling frequency of 107795 MHz.*

By comparing the results from the measurements with different antenna frequencies, a better spatial resolution is observed for the higher frequencies. The zone which was influenced by the electromagnetic wave was smaller for these frequencies. From the single tree profile measurements the greatest diameter for this zone was estimated, and by using the Fresnel zone concept a theoretical value was derived (Table 1).

Table 1. *Approximate values of the electromagnetic influence zone estimated from single tree measurements and derived from the Fresnel zone approach for three different antenna frequencies.*

Antenna frequency (MHz)	Estimated diameter of the influence zone (m)	Diameter of the Fresnel zone (m)
200	1.0	0.97
500	0.7	0.61
800	0.5	0.48

The detected amplitude changes with the 800 MHz antennas and the estimated conductivities for the single tree profile measurements are presented below (Figure 15). As the amount of water on the tree was raised in a first step an increase of amplitude and decrease in conductivity can be observed. The greatest changes occurred at distances around 0.4 m and 1.3 m. When the water amount was raised a final time, greater changes in amplitude and conductivity were only determined at the top of the tree and the lower end of the tree. The results showed a decreasing amplitude at these levels leading to an increase in conductivity.

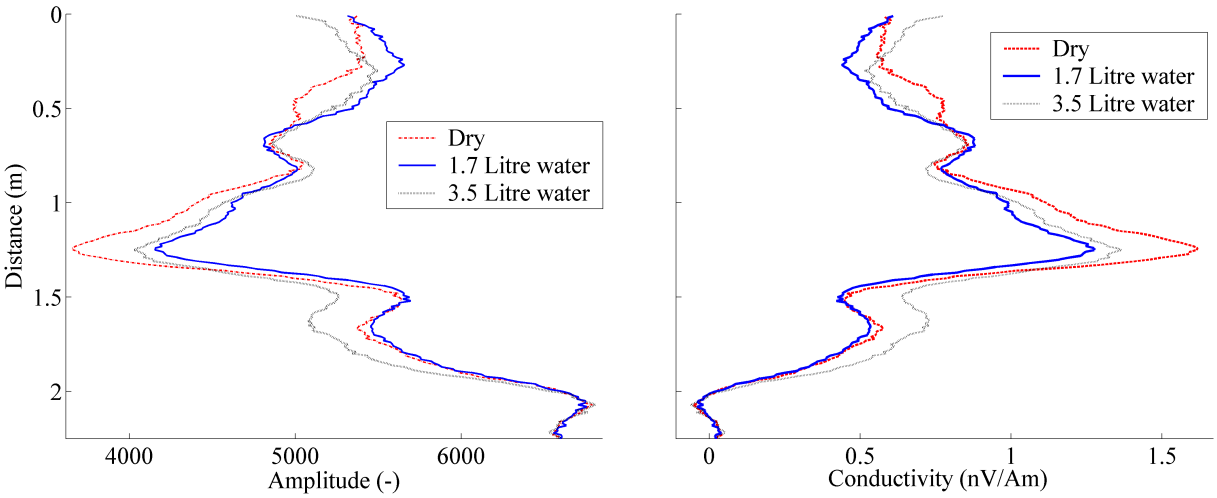

Figure 15. *Measured amplitudes (left panel) and estimated conductivities (right panel) from single tree profile measurements, from the top of the tree (0 m) to its lower end (~1.7 m), with different amounts of water on the tree, using an 800 MHz shielded antenna.*

3.1.3. Experimental evaluation of mixing formulas

From the single tree profile measurements amounts of intercepted water (kg/m^2) were estimated. These values times the approximate area occupied be the lower end of the spruce was interpreted as the mass of water on the tree (Figure 16). An overestimation by a factor 2.7 can be observed comparing the reference weights measured with the scale and the estimated mass of water from the radar measurements using an 800 MHz shielded antenna.

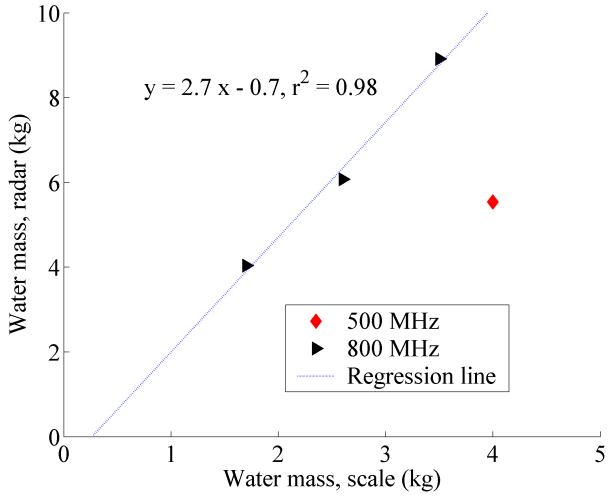

Figure 16. *Water weights measured with a scale and amounts of water estimated from radar measurements for single tree profile measurements, using 500 and 800 MHz antenna frequencies.*

During the measurements performed on the bunch of hanging spruce branches, using the 800 MHz antennas, the impulse wave velocities decreased as water was poured on them (Figure 17). With time after the wetting occasions a small increase of the wave speed was estimated, more marked after the second occasion, which seems to follow an exponential trend. Translating the velocity changes into fractions of water and then rescaling the results to amounts of water using the Fresnel volume concept to the assumed actual measured volume gave an overestimation with ~132% compared to weights captured with the scale.

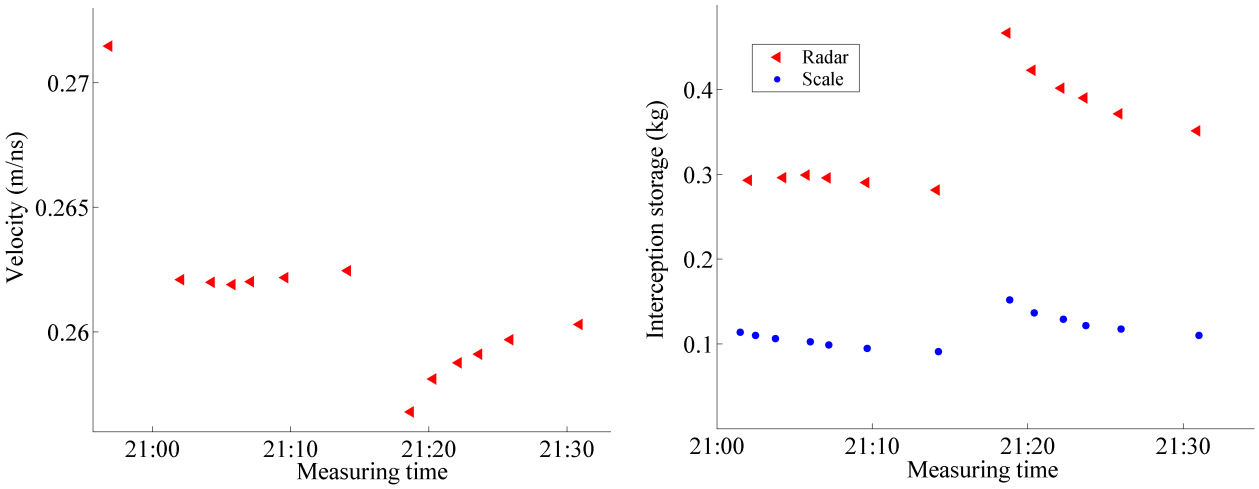

Figure 17. *Impulse wave velocities (left panel) and amount of intercepted water (right panel), derived from measurements on the bunch of hanging spruce branches, using an 800 MHz shielded antenna. The first measured velocity, before 21:00, represents the dry branches. At two separate occasion, around 21:02 and 21:18, water was poured on the branches. From the velocity values amounts of water were estimated and presented with the scaled weights.*

3.1.4. Attenuation with distance

The forest measurements in Malå shows an exponential amplitude decrease with an increasing antenna separation (Figure 18). Significant differences between the amplitude values detected by the two antennas can not be observed. The higher frequency measurements has a greater amplitude-to-noise ratio than the lower frequency measurements, especially as the antenna separation increases.

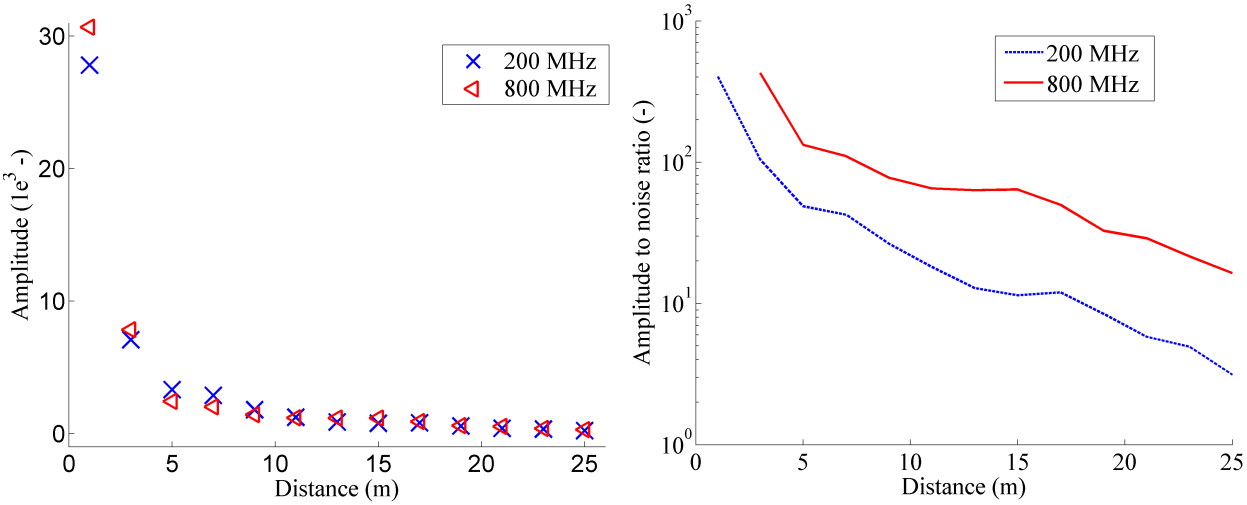

Figure 18. *Actual measured amplitudes (left panel) and estimated amplitude-to-noise ratios (right panel) with 200 and 800 MHz antenna frequencies at different distances between the transmitting and receiving antennas.*

3.2. Field experiments

The profile measurements taken under the field experiments all had several common features, which are exemplified in the radargram of the measurement 18 January 17:00 (Figure 19). The

sampling frequency was moderate (33042 MHz) and the time window relative wide, which allowed secondary impulse waves to being detected. Except the first arriving pulse traveling on a straight path between the antennas, two secondary pulses can clearly be identified in this radargram. One clear and strong impulse representing the ground reflection and one weaker, likely from a metal device attached at one of the masts. The amplitude and the contrast of the ground reflection increased, and its travel time naturally decreased as the antennas were moved downwards.

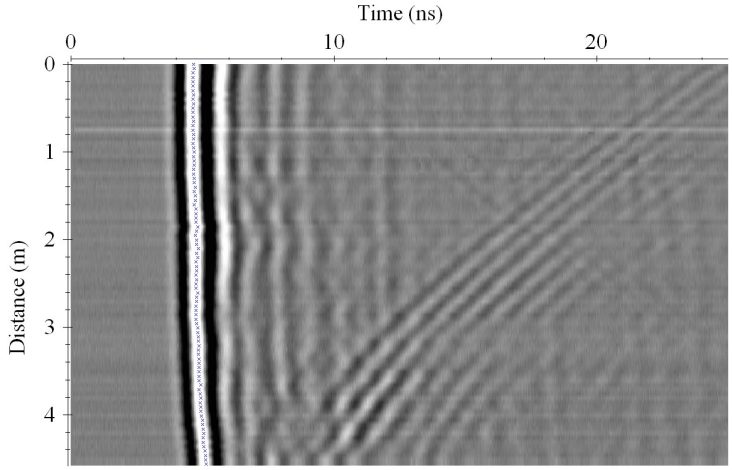

Figure 19. *Radargram from one vertical profile measurement of the forest section, from above the trees (0 m) and downwards towards the snow surface. Bright areas represent positive amplitudes on the impulse wave and dark regions represent negative amplitudes. The first arrival times interpreted for the impulse waves are marked with crosses.*

No changes of the impulse wave travel time or its amplitude could be detected as the cables used during the field measurements were moved to test these drifts. Drifts only occurred as the connections were dislodged, equal in magnitude to those detected during the laboratory tests.

From the forest stand radargram above the impulse wave velocities were derived (Figure 20). Three further velocity profiles distributed over three days are presented along the corresponding estimated changes in water fraction with respect to the first measurement. Notable are the velocity changes around the distance 2 m during the second day. In the morning. the impulse wave suffered a slight velocity decrease compared to the evening before, but in the afternoon it had turned faster again. At the last measurement 19 January, a velocity decrease over the complete profile was observed compared to the reference measurement 18 January. These variations resulted in changes of water fractions over the period with a significant raise for the last measurement.

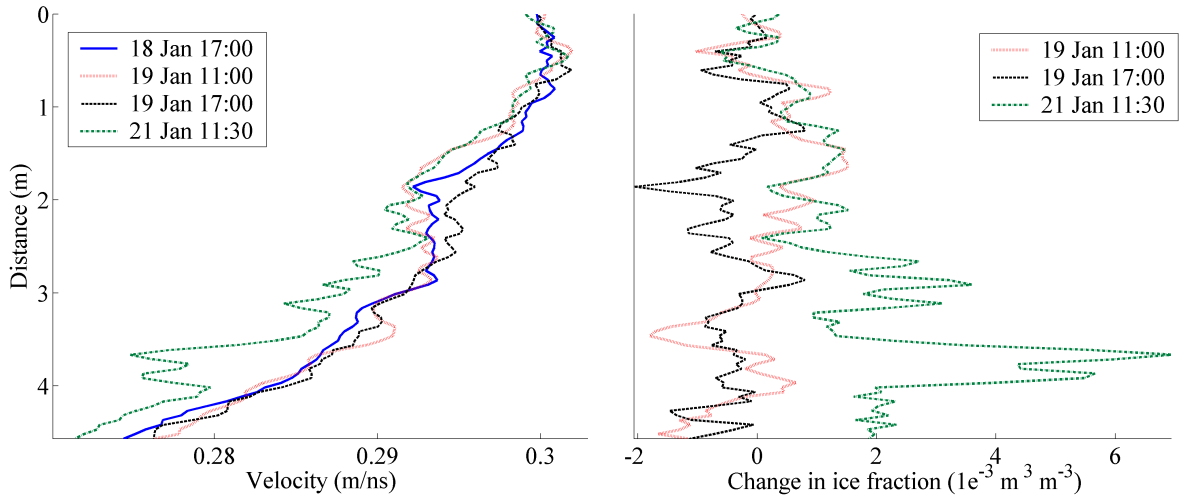

Figure 20. *Impulse wave velocities (left panel) and changes in ice fraction with respect to the first measurement performed (right panel), derived from profile measurements of the forest section, from above the trees (0 m) and downwards, using an 800 MHz shielded antenna. Changes in ice fractions are estimated from the presented velocity profiles.*

The detected amplitudes and the estimated conductivity changes from the first measurement occasion are presented below (Figure 21). Only small changes for these quantities can be seen over the measured period. From the first to the second day a slight decrease in amplitude was detected over most parts of the profile. A further decrease in amplitude can be observed at the last occasion. The changes in conductivity with respect to the first measurement follows inversely the measured amplitudes.

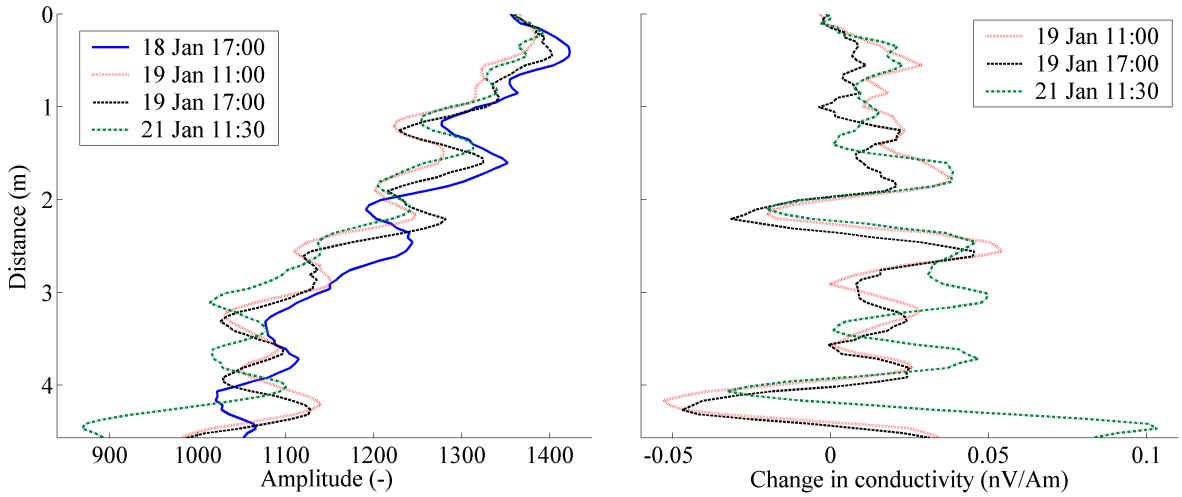

Figure 21. *Measured amplitudes (left panel) and estimated changes in conductivities with respect to the first measurement (right panel), from profile measurements of the forest section, from above the trees (0 m) and downwards, at four different occasions, using an 800 MHz shielded antenna.*

The volumetric contents of ice determined from the radar measurements and the measured weights of the tree were transformed into a comparable estimate of the interception storage (kg/m^2) (Figure 22). The measurement with the tree weighing device started in the evening of the third day (20 January), at the same time as the onset of a snowfall that continued during the night. The weight of the tree increased with about 5 kg during the night.

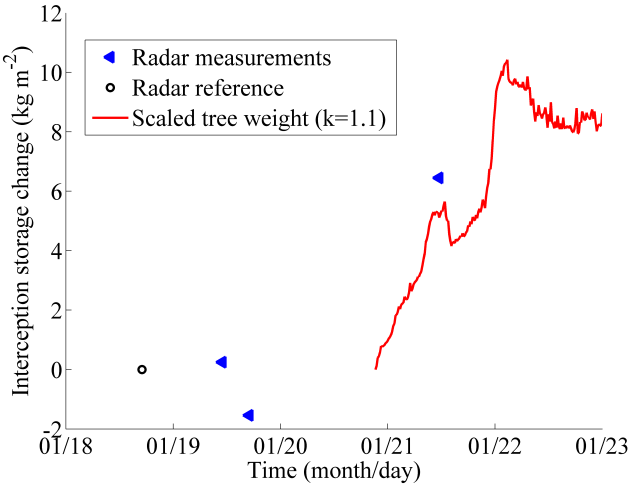

Figure 22. *Changes in interception storage, in relation to a reference measurement (18 January), estimated from radar results and determined from the tree weight measurements.*

The radar measurements after snow was shaken of the trees indicated that the impulse wave velocities were further decreased, which was not expected since the interception storage clearly was reduced (Figure 23). The fastest velocities were observed as the snow still was laying on the forest, measured at 17:00. A decrease in velocity over the profile was the result after the two rounds as snow was shaken of the trees, measure at 17:10 and 17:20. From a velocity decrease an increase in fraction of ice is given when applying the mixing formulas used in this study.

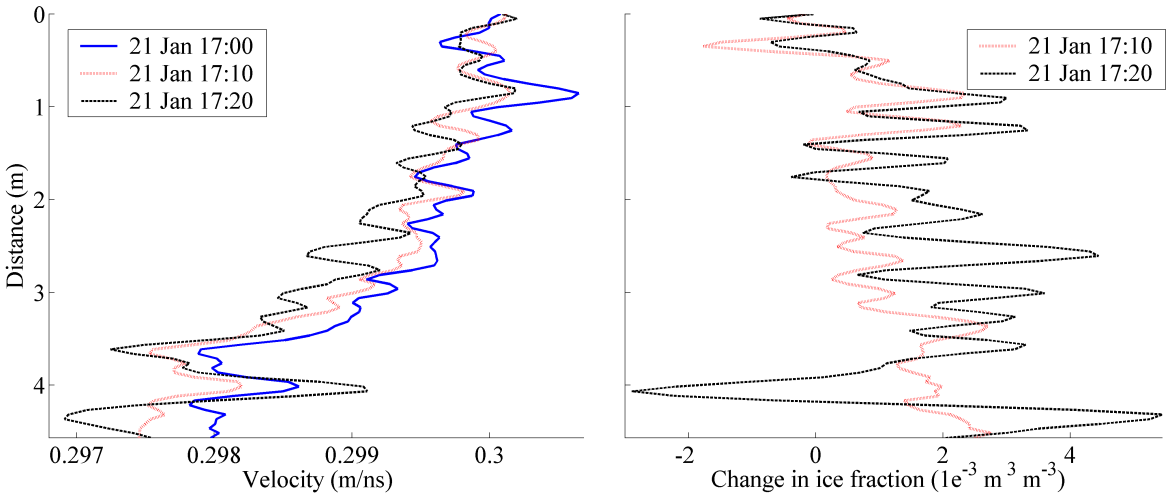

Figure 23. *Impulse wave velocities (left panel) and changes in ice fraction in respect to the first measurement performed (right panel), derived from profile measurements of the forest section as snow was shaken of the trees, from the top of the trees (0 m) and downwards, using an 800 MHz shielded antenna. Changes in ice fractions are estimated from the presented velocity profiles.*

Detected amplitudes and estimated conductivities as snow was shaken of the trees are presented below (Figure 24). Generally, amplitudes were decreasing all the way from the top of the tree towards to the ground as snow still was on the trees. After the snow was shaken of the trees a significant rise in amplitude was detected, indicating lower attenuation losses. Thus, a decrease of the conductivity compared to the first measurement could be estimated.

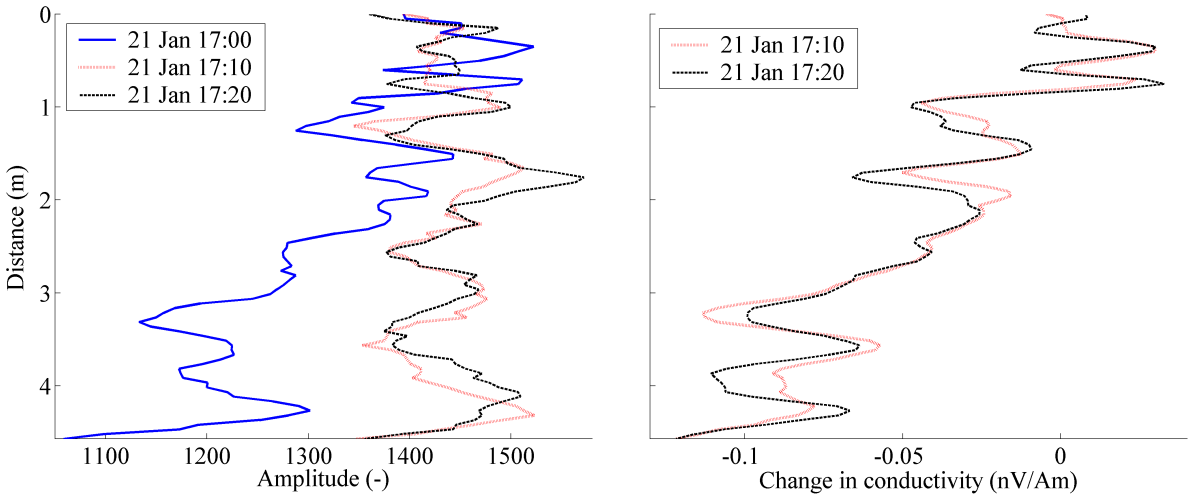

Figure 24. *Measured amplitudes (left panel) and estimated changes in conductivities in respect to the first measurement (right panel), from profile measurements of the forest section, from the top of the trees (0 m) and downwards, as snow was shaken of the trees, using an 800 MHz shielded antenna.*

4. Discussion

4.1. Laboratory tests

The small but significant drifts in the timing of the equipment showed that continuously performed reference measurements in air were necessary to achieve reliable results. After the initial warm-up phase the output values stabilized, were moderate and foremost considered predictable, following approximately linear relations over short time intervals. This implied that drifts over time could be compensated for to avoid systematic errors in the measurements. Random variations caused by cable movements and dislodging of connections was probably a minor problem in the laboratory tests. However, it can be a serious problem for applications with moving radar antennas, such as the forest stand profile measurements performed in the field scale tests.

The variation of impacts of a tree or not compared to the additional intercepted water illustrated the importance of choosing an appropriate sampling frequency and time window to capture all changes with a sufficient high accuracy. Even the slight increase for the travel time of the impulse wave caused by one small canopy was detected by the radar system, for instance visible in the radargram presented in Figure 12. The velocity profile (Figure 13) determined from the travel times shows this effect even clearer, where small velocity variations can be interpreted as changes in thickness of the canopy. Water poured on the tree resulted in slower advancing pulse waves due to a raised dielectric constant, which is in line with what was expected from theory. The form of the velocity curves were slightly changed as the dry tree was wetted, probably caused by changed branch architecture due to the heavier load. From the fractions of water, estimated from the impulse wave velocities, one can observe that the tree at the first occasion was wetted more at its top, and at the end more at its lower part. Velocity decreases due to a raised water storage on the tree could not be detected with the 200 MHz antenna (Figure 14), an effect likely depending on a greater part of the impulse wave taking travel paths around the tree or through air space inside the canopy, completely unaffected by the water. The fraction of the impulse wave actually affected by the water was probably masked by the other pulses.

With the two higher frequency antennas, especially the 800 MHz variant, a better spatial

resolution of the tree was observed for the profile measurements of the single spruce compared to the low frequency antenna. Both antennas were shielded, which means that the spreading of the generated impulse wave is reduced compared to unshielded antennas. Furthermore, higher frequency waves are expected to be affected by a smaller volume surrounding the direct travel path, which can explain the observed behavior of the different antennas. The experimentally estimated diameter on the cross-section of the Fresnel volume and the theoretically derived results shows a good agreement (Table 1).

The amplitude curves depicted (Figure 15) for the profile measurements of the single spruce were harder to interpret than the velocity results. Spatial variations were less distinct and the form of the amplitude curves differed significantly to the velocity profiles, indicating other factors influencing the impulse wave attenuation than its velocity. By intuition, it is expected that a raised water storage on the canopy brings greater ohmic energy losses causing larger attenuation, induced by an increased conductivity. From eq. (19) a fall in amplitude is only predicted if the decrease in impulse wave velocity is greater than its increase in conductivity. Since the velocity depends on the dielectric constant and this constant is around 25 times larger than the conductivity for water the detected amplitude variations are in principle possible. However, the estimated conductivities contradict this line of arguments. One explanation can be that the conductivities do not follow a continuously increasing relation to the amounts of water pored on the trees, perhaps due to structure dependent properties. The simplified medium description and assumptions made on the electromagnetic impulse wave could be another reason. A third explanation could be that the wetted tree acts like a lens, redirecting the electromagnetic rays towards the receiving antenna. This is definitely an area that needs more attention, especially since the combination of measurements of attenuation and dielectric constants might be a way to separate liquid and frozen interception.

The estimated storage of water translated from the velocities achieved during the single tree profile measurements and the experiments performed (Figure 16) on the bunch of hanging spruce branches (Figure 17) showed an overall overestimation compared to independent measurements with the scale. This discrepancy indicated that structure independent mixing formulas may not really be applicable to such small and relatively uneven test samples. Looyenga's relation is based on the assumption that all components of the medium are randomly distributed, which might be one reason for the differing results. The water poured on the tree and the branches was not evenly distributed either, leading to an incorrect scaling of the estimated water fractions into amounts of water. However, still it was interesting to observe the exponential decay in water storage with time estimated both from the radar measurements and captured with the scale. Thus, the experiment on the bunch of hanging spruce branches showed that variations of the interception storage very well could be captured by the radar method. A similar observation could be made from Figure 16 were the water weights estimated from the results captured with the 800 MHz antenna and the scale measurements showed a good agreement of variations. Although, to few measurements makes conclusions uncertain.

The amplitude decrease with distance in the forest (Figure 18), following an exponential trend, depend mainly on geometric energy losses but probably also due to increasing amount of woody material between the antennas. The amplitude for the 200 MHz antenna were lower than could be expected since an unshielded antenna radiates higher energy levels then the shielded variants. Probably, the low elevation of the antennas compared to the separation distance implied a greater impact on the lower frequency impulse wave from the ground due to its greater zone of influence. The most important result of these tests were the promising test with the 800 MHz antenna. Even at antenna separations of around fifteen meters a clear signal could be detected, illustrated by the estimated amplitude-to-noise ratios. This is probably a minimum required antenna separation in order to be useful for representative measurements at the forest stand level.

4.2. Field experiments

Two reflections, one from the ground and one from some surrounding object, and the direct travel path from transmitter to receiver of the impulse wave could be interpreted from the radargram presented in Figure 18. Commonly, as in this case, several pulses can be spotted in a radargram and it can be difficult to interpret and to pick those pulses who are considered interesting. One problem often arising, which is important for these measurements, are pulses traveling around objects faster and arriving at the same time or earlier than those taking the shortest direct path. The signal which is of interest is then disturbed by the faster and differently attenuated pulses. It may even be hard to interpret from the radargram. In a dense forest, especially at the lower part of trees, possible travel paths like these seem unlikely. Studying the radargrams obtained in this study, no pulses with higher or similar amplitudes were detected arriving after the first arrival. Therefore, the issue of round-about pulses was not considered as a major problem during these measurements due to the dense forest between the antennas. However, the method may not be suited for measurements performed in thin forests for this reason.

A more problematic feature of the current measurements was that no distinct leap of the impulse wave speed from air to canopy air space could be detected at the upper end of the profiles. Thus, it was difficult to establish a well defined air reference which is used to correct for drifts in the system, and make the time zero correction of the measured first arrival times. The starting position of the measurements was just above the tree-tops, and the corresponding Fresnel volume was probably influenced by the upper parts of the canopy already at this point.

Despite the uncertainties and imperfect installation, the results of snow interception storage were promising and logical with regard to the observed weather conditions and the weighted tree reference. First, the estimated velocity variations and corresponding changes in the interception storage between the 18 and 19 January could be an effect of the white frost formation that was observed on the trees during the night. The radar measurements suggested an increase of the estimated snow storage during the night, and a decrease during the day, which could be an effect of a much likely evaporation at the upper part of the canopy. Secondly, the last measurement on the 21 January captured the snow fallen during the night as a decrease in velocity giving an increasing amount of ice which was in the same range as the estimate based on the weighted tree.

The last measurements after snow was shaken of the trees gave perhaps the only unexpected results concerning the impulse wave velocities. The decreasing impulse wave velocities as the snow on the trees was shaken of contradicts the theory presented in this paper. Likely it depends either on geometry changes of the trees influencing the impulse wave speed or on the unsuccessful radar installation. If the antennas were not raised high enough the air reference was certainly affected, leading to uncertain results. The amplitude changes over the measurements are clear and would support the theoretic approach presented.

4.3. Measurement uncertainties

The uncertainty analysis was rough and oversimplified. For example, regard has not been taken to the signal processing steps, which improved the accuracy of the travel time determinations. Other uncertainties, due to equipment imperfections among others, are assumed to be smaller than the used estimations.

During the laboratory tests all uncertainties from movements, as varying antenna separations of the equipment were prevented. Only the sampling frequency was assumed to influence the accuracy. The changes determined for the velocities, water fractions and amounts of water were commonly larger than the highest estimated uncertainty. From these observations it can be concluded that a sufficient high accuracy can be achieved with the radar system to resolve such

small changes as the velocity decrease induced by a raised water amount on a single tree.

Measurement uncertainties caused by the radar equipment itself were assumed to be small at high sampling frequencies, especially at great antenna separations, compared to those due to the antenna movements, and then foremost horizontal dislocations. Results from the field experiments can generally be considered as unreliable due to the high estimated uncertainties. On the other hand, the analysis performed gave the lowest expected accuracy. In reality the uncertainties could be smaller then those predicted. At least it can be concluded that, with a sufficient stable construction, these uncertainties can be reduced to an acceptable level.

There were no straight forward ways to estimate the uncertainties for the amplitudes, why such an analysis was omitted.

4.4. Operational setup

Some requirements for a final transmission installation can be stated as follows:

- The 800 MHz shielded antenna should be preferred of those tested in this study, since it achieved both a better spatial resolution and a higher accuracy for the wave travel time.
- Designing a stable construction, where especially only very small horizontal antenna dislocations are possible.
- Using optic cables with reinforced lining to prevent drifts caused by cable movements.
- Automate the system and use a steady power supply for the control unit and the antennas.
- Starting and finishing every profile measurements of the forest section with the antennas raised several meters above the trees to determine a certain air reference. Compensating measured times and amplitudes of the impulse wave with a curve interpolated from these points.
- Using a high sampling frequency, the widest possible antenna separation and improve the signal processing.

5. Conclusions

Impulse radar can be used to measure the snow interception storage in coniferous forest stands with both high temporal and spatial resolution. However, an appropriate installation and a better theoretical understanding of the electromagnetic properties of a forest canopy is needed to achieve high accuracy and to avoid the need for empirical calibration of the method. In particular, the conclusions of this study were that:

- The laboratory experiments showed that the influence of liquid water interception on the electromagnetic properties of a single tree canopy was well above the detectable limits of the radar system, with respect to both attenuation and velocity changes.
- The field experiments showed a good agreement between estimated changes of the interception storage and observed weather variations and reference measurements using a tree weighing device, all in spite of a non-optimal equipment installation.
- Estimations of the mass of intercepted water based on Looyenga's mixing formula and velocity changes overestimated the intercepted storage of water with respect to reference measurements. A small heterogeneous test sample with an uneven distribution of water could be one explanation for this. The observed difference between the estimated water amounts from radar measurements and measured weights is considered to be a systematic

overestimation as relative variations were well captured.

- No clear empirical relation between amount of water and conductivities, estimated from the impulse wave attenuation could be found. These results were difficult to interpret, and appropriate mixing formulas were not found in literature. Further studies concerning this area are of interest.

Long-term interception measurements in the field have to be performed using a well functioning installation, in order to further evaluate and improve the impulse radar method. The validity of mixing formulas can then be examined further, again by comparing the amount of intercepted snow determined from the radar measurements to independent estimates of the interception storage. For example, with a large antenna separation the assumption of randomly distributed medium components used for mixing formulas can be considered valid. This approach would also really prove whether a varying interception storage of snow actually can be detected by impulse radar system with high enough accuracy, and if the criteria for an ideal measurement method presented in the introduction section can be met.

6. References

Albert, M., Koh, G. & Perron, F. (1999). Radar investigations of melt pathways in a natural snowpack. Hydrological processes, 13, 2991-3000.

Angot, L., Roussel, H. & Tabbara, W. (2002). A full wave three dimensional analysis of forest remote sensing using VHF electromagnetic wave. Progress In Electromagnetic Research, PIER 38, 311-331.

Annan, A. (2003). Ground Penetrating Radar, Principles & Applications. Sensors & Software Inc.

Bosch, J. & Hewlett, J. (1982). A review of catchment experiments to determine the effect of vegetation changes on water yield and evaporation. Journal of hydrology, 55, 3-23.

Bouten, W., Swart, P. & Dewater, E. (1991). Microwave transmisson, a new tool in forest hydrological research. Journal of hydrology, 124, 119-130.

Bruland, O. (2002). Dynamics of the seasonal snowcover in the arctic. (Ph.D. Thesis, Department of Hydraulic and Environmental Engineering. Norwegian University of Science and Engineering.)

Essery, R., Pomeroy, J., Parviainen, J. & Storck, P. (2003). Sublimation of snow from coniferous forests in a climate model. Journal of climate, 16, 1855-1864.

Fletcher, N. (1970). The chemical physics of ice. Cambridge University Press.

Frolov, A. & Macharet, Y. (1999). On dielectric properties of dry and wet snow. Hydrological processes, 13, 1755-1760.

Hedstrom, N. & Pomeroy, J. (1998). Measurements and modelling of snow interception in the boreal forest. Hydrological processes, 12, 1611-1625.

Johnson, T., Routh, P. & Knoll, M. (2005). Fresnel volume georadar attenuation-difference tomography. Geophys. J. Int., 162, 9-24.

Lundberg, A. & Halldin, S. (2001). Snow interception evaporation. Review of measurement techniques, processes, and models. Theoretical and applied climatology, 70, 117-133.

Lundberg, A., Calder, I. & Harding, R. (1998). Evaporation of intercepted snow: measurement and modelling. Journal of hydrology, 206, 151-163.

Mathworks (2006). http://www.mathworks.com/access/helpdesk/help/toolbox/signal/signal.html (2006-04-12)

McNay, R., Peterson, L. & Nyberg, J. (1988). The influence of forest stand characteristics on snow interception in the coastal forests of British-Columbia. Canadian journal of forest research-revue, 18, 566-573.

Pfister, R. & Schneebeli, M. (1999). Snow accumulation on boards of different sizes and shapes. Hydrological processes, 13, 2345-2355.

Råde, L. & Westergren, B. (1998). Mathematics Handbook for Science and Engineering. Studentlitteratur.

Sahin, V. & Hall, M. (1996). The effects of afforrestration and deforrestration on water yields. Journal of hydrology, 178, 293-309.

Sihvola, A. (1999). Electromagnetic Mixing Formulae and Applications. London: Institution of Electrical Engineers.

Spetzler, J. & Snieder, R. (2004). The Fresnel volume and transmitted waves. Geophysics, 69, 653-663.

Wangsness, R. (1986). Electromagnetic Fields. 2nd ed., John Wiley & Sons Inc.

Young, H. & Freedman, R. (2000). University physics. 10th ed. Addison-Wesley publishing company.

Zakri, T., Laurent, J. & Vauclin, M. (1998). Theoretical evidence for ´Lichtenecker's mixture formulae´ based on the effective medium theory. J. Phys. D: Appl. Phys., 31, 1589-1594.